U.PORTO
FEUP FACULDADE DE ENGENHARIA
UNIVERSIDADE DO PORTO

University of Porto

Faculty of Engineering

Analysis of stationary periods during the Perdigão 2017 campaign

João Pedro Donas Boto Carvalho

Supervisor: Doutor Alexandre Silva Lopes

Dissertation submited to the University of Porto
in partial satisfaction of the requirements for the
degree of Master in Mechanical Engineering.

June 2019

Contact information:
João Pedro Donas Boto Carvalho
email: up201305897@fe.up.pt

This document was typeset with LaTeX using the **CVR** thesis template.

Abstract

The main purpose of this thesis was on the analysis of stationarity in the measurements of the Perdigão 2017 field experiment. The three velocity components of the wind flow, measured by several sonic anemometers mounted at various heights in three towers (two 100 m and one 60 m high), were analyzed during the entire intensive observation period (IOP), from May 1 to June 15, 2017.

To identify the stationary periods, the data was submitted to a sequence of tests. The first one tested the wind direction and periods where the wind was normal to the hills and larger than 30 min were gathered. Then, the resultant velocity fields were rotated to a reference frame aligned with the incoming wind, which were then considered in the tests that followed.

The second filter considered the integral time scale of the three velocity components and intended to eliminate time series with a low-frequency component, associated with the passage of large eddies. Next, the time series was divided into 3 min periods and the following tests attempted to determine whether consecutive periods could be considered to have the same statistical properties. The first was the reverse arrangements test, with the goal of removing time series with an underlying trend.

In order to complete the procedure, the 3-min periods were submitted to a hypothesis test, to check if they had the same average, and the Kolmogorov–Smirnov test, to verify if they had the same statistical distribution. The goal was to join all the consecutive periods that could be considered to have the same properties and find the longest time series that could be considered stationary. These series were also subjected to a criterion based on the nonstationarity ratio, which was already applied to atmospheric flows.

For NE winds, the day which represented better results was May 23, between 21h and 23h. For SW winds in the south ridge, May 4 presented stationary conditions between 21h and 23h, at 60, 80 and 100 m height. Also, on May 9, between 21h30 and 24h, several periods were found with the same average and distribution. On May 26, all towers registered stationary conditions, but not coincident in time. Finally, on May 29, stationary periods were found between 1h and 2h and even more from 3h30 to 4h30, in tower 20 at 20–60 m height.

Resumo

O objetivo principal desta tese foi a análise da estacionariedade nas medições da experiência de Perdigão 2017. Os três componentes de velocidade do vento, medidos por vários anemómetros sónicos montados a diversas alturas em três torres (duas de 100 m, uma de 60 m de altura), foram analisados durante todo o período de observação intensiva (IOP - Intensive Observational Period), de 1 de maio a 15 de junho de 2017

Para identificar os períodos estacionários, os dados foram submetidos a uma sequência de testes. O primeiro testou a direção do vento, e os períodos em que não era normal às colinas por, pelo menos 30 min, foram rejeitados. Em seguida, os campos de velocidade resultantes foram rodados para um referencial alinhado com o vento incidente, para serem considerados nos testes que se seguiram.

O segundo filtro considerou a escala de tempo integral dos três componentes de velocidade, e pretendia eliminar as séries temporais com uma componente de baixa frequência, associada à passagem de grandes escalas. Em seguida, a série temporal foi dividida em períodos de 3 min e os testes a seguir tentaram determinar se períodos consecutivos poderiam ser considerados como tendo as mesmas propriedades estatísticas. O primeiro foi o teste de arranjos inversos, com o objetivo de remover séries temporais com uma tendência subjacente.

Para completar o procedimento, os períodos de 3 min foram submetidos a um teste de hipóteses, para verificar se tinham a mesma média, e ao teste de Kolmogorov–Smirnov, para verificar se tinham a mesma distribuição estatística. O objetivo era juntar todos os períodos consecutivos que podessem ser considerados como tendo as mesmas propriedades e encontrar séries temporais tão longas quanto possível que pudessem ser consideradas estacionárias. Estas séries também foram também submetidas a um critério baseado no rácio de não-estacionariedade, que já foi aplicado anteriormente a escoamentos atmosféricos.

Para os ventos de noreste, o dia que representou melhores resultados foi o 23 de maio entre as 21h e as 23h. Para os ventos de sudoeste, na cordilheira sul, o 4 de maio entre 21h00 e 23h00 apresentou condições estacionárias, a 60, 80, 100 m de altura. Em 9 de maio entre as 21h30 e as 00h00, onde foram encontrados vários períodos com a mesma média e distribuição. No dia 26, todas as torres encontraram condições estacionárias, mas não coincidiram no tempo. Finalmente, em 29 de maio, os períodos estacionários entre 01h e 02h, ainda entre 03h30 às 04h30, foram encontrados na torre 20 a 20-60 m de altura.

Acknowledgements

I would like to thank my thesis advisor Doutor Alexandre Lopes for his patience and guidance. He always provided valuable comments and assistance, as well as recommendations and several revisions throughout the semester.

I also want to thank Prof. José Laginha Palma for the invitation to join this project. He consistently allowed this thesis to be my own work and steered me in the right direction providing guidance and knowledge. I would also like to thank Vítor Gomes and Carlos Silva for their constant advice, suggestions and to provide a very pleasant environment to work on this thesis.

This work would not have been possible without the financial support of the Portuguese Foundation for Science and Technology (FCT), under research project NEWA – New European Wind Atlas (NEWA/0001/2014), which permitted the Portuguese participation in the Perdigão 2017 campaign.

I am thankful to all my friends who allowed me, during the faculty, to handle all my challenges in a better way.

Finally, I give my warmest thanks to my family for the continuous support and everything that they provided me along the years and Carito for her continuous encouragement. This accomplishment would not have been possible without them.

Table of Contents

List of Figures

List of Tables

Nomenclature

Greek symbols

α	Level of significance	[%]
η	Time interval, used in correlation function	[s]
μ	Mean of random variable	
ϕ	Generic variable	
ρ_ϕ	Autocorrelation function of a generic variable ϕ	
σ^2	Variance of random variable	
τ_ϕ	Integral time scale of a generic variable	[s]
τ_u, τ_v, τ_w	Integral time scale of the streamwise, spanwise and vertical velocity components	[s]

Roman symbols

$C_{\phi\phi}$	Correlation function of a generic variable ϕ	
H_0	Null hypothesis	
H_1	Alternative hypothesis	
N	Number of records of each time series	
NE	Northeastern	
SW	Southwestern	
TS	Test statistic	
u, v, w	Streamwise, spanwise and vertical velocity components	[m s^{-1}]
x, y, z	Local coordinates	[m]
x_i	Represents a certain i subset	

5

Chapter 1

Introduction

1.1 Perdigão campaign

The Perdigão field campaign is part of large joint US/European program. The campaign will help to provide the wind industry with thorough resource mapping proficiency in the form of a New European wind atlas, NEWA project (Mann, 2015).

In this large project a standard for site assessment will be developed, based on improved modelling competencies on atmospheric flow. Several European research groups were involved, which seek to develop new dynamic methodologies of downscaling, as well as using the measurements with high temporal and spatial resolution to improve existing models.

The Perdigão campaign took place from 15 December 2016 to 15 June 2017 which was divided in two events:

- Extensive Measurements Period (EMP) — 15 December 2016 to 30 April 2017
- Intensive Observational Period (IOP) — 1 May to 15 June 2017

A few groups of American researchers have also joined this project. This collaboration allowed the utilization of a larger amount and variety of instrumentation than in previous experiments, e.g. "The Askervein hill project" (Taylor and Teunissen, 1987), used to make measurements with high spatial resolution which, thereby, made it known as the world's largest wind-mapping experiment ever performed (Witze, 2017).

The main purpose of Perdigão campaign is to get a set of measurements (database) that allow the development and improvement of the numerical models which better represent flow over complex terrain than those currently in use. In the US context, the focal points will be to use these data to understand complex terrain physical and thermodynamic processes and create new models that better represent the physics of flow over complex terrain (NCAR/UCAR, 2016). In the context of the FEUP group, mainly interested in numerical modelling, this work tried to supply reliable data for the development and validation of models.

1.2 Description of site and instrumentation

The Perdigão site was an ideal place to study an atmospheric flow with separation, the major interest in its selection was based on:

- the double parallel ridge topography with southeast-northwest orientation;
- approximate ridge-normal direction annual wind climatology;
- horizontally isotropic turbulence;
- data available from a 100 m mast;
- topographic complexity, with forested hilly terrain.

There is also a wind turbine, located on the southern ridge, which allows the study of the wake flow and its interaction with the second ridge, plus power output dependence on atmospheric conditions (da Silva, 2018).

1.2.1 Instrumentation

The plurality of participating research groups permitted deployment of dense arrays of instruments to examine the microscale of atmospheric structure. Previous results allowed to delineate the best locations of those instruments. To reach the various scientific objectives, 49 towers, 18 scanning and 8 profile lidars were installed in the field, to measure the wind velocity, along with instruments to measure other quantities.

The concern of this study was to take data from three of the towers, two 100 m high towers (`20/tse04` and `29/tse09`) and one 60 m high tower (`37/rsw06`). These towers are highlighted with white circles in Figure 1.1. All of them were placed on top of the ridges in order to analyze the upstream and downstream wind flow over the hills. The towers `20/tse04` and `29/tse09` were located in the same line of action, approximately in the campaign domain centre, but at different ridges.

Each tower was constituted by three-component sonic anemometers, temperature/humidity sensors, barometers, radiometers, gas analyzers, wetness sensors, heat/moisture flux sensors, thermo-hygrometers, and three pyrgeometers (Fernando et al., 2018). In the studied towers, the instruments were mounted at heights between 10 and 100 meters, per every 10 meters above ground level.

Appendix A includes the location of each tower and the devices used to measure the flow velocity.

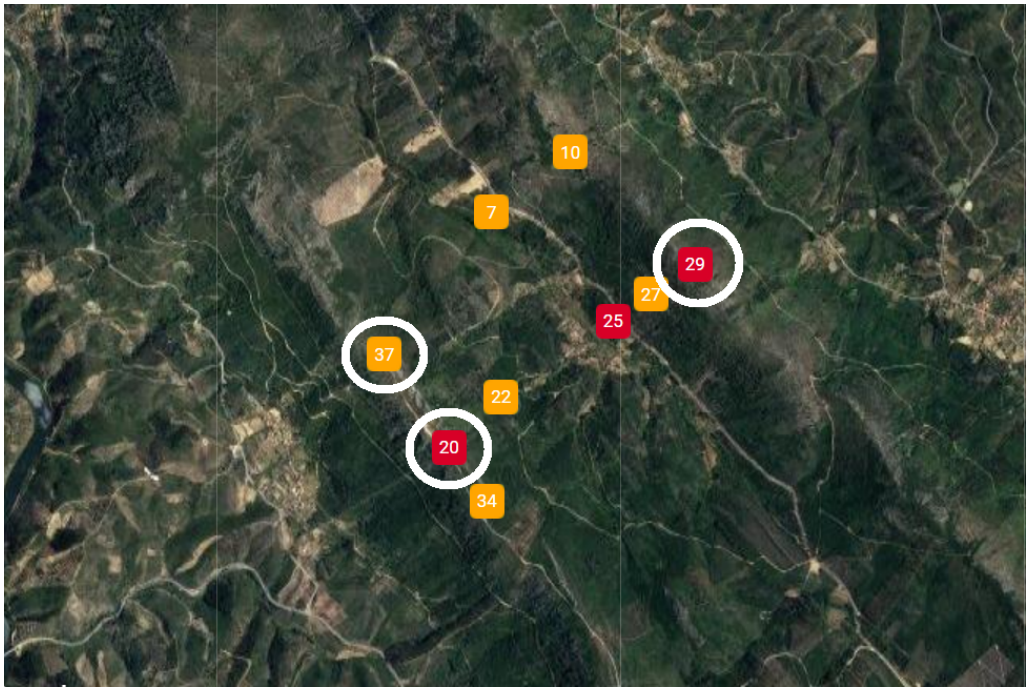

Figure 1.1: Reference points location (yellow points are the 60 m towers and red points are the 100 m towers

1.2.2 Data collection and user access

NCAR's NIDAS software collected all tower data in real-time, through an extensive WiFi network, which was uploaded to the Earth Observing Laboratory (EOL, United States), the University of Porto (UPORTO, Portugal) and the Technical University of Denmark (DTU, Denmark) repositories. The archives were periodically synchronized and kept consistent.

The data, obtained during the IOP (Intensive Observation Period) of the Perdigão 2017 campaign, are available in three different archives (Fernando et al., 2018):

- UPORTO (http://perdigao.fe.up.pt)
- UCAR (https://www.eol.ucar.edu/field_projects/Perdigao)
- EU (http://www.neweuropeanwindatlas.eu)

under the responsibility of research groups in Portugal (University of Porto, Faculty of Engineering), in the USA (NCAR, National Center for Atmospheric Research) and in the Denmark (DTU, Technical University of Denmark).

The anemometers used a sampling frequency of 18 Hz and the data were compressed and stored in sequences of 10 min, identified with the start date and time. In the present work, the towers' data were downloaded from http://perdigao.fe.up.pt through a function executed in Matlab software which extracted the raw data. All these files had multiple variables but the Matlab's function only organized the data by the horizontal and vertical speeds for the towers number 37,29 and 20 and for each corresponding height.

1.3 Objectives and motivation

The main objective of this dissertation is to identify the largest time periods which the wind velocity, measured in a tower at a certain height, can be considered statistically stationary.

In the Intensive Observation Period (IOP), from the 1st of May to the 15th of June 2017, measurements were explored in order to indicate time periods when the wind flow over the ridges had been stationary.

We expect that this, combined with other research works, will help to increase the knowledge about atmospheric flows and contribute to the improvement of wind energy technologies and applications.

1.4 Outline of the thesis

This dissertation is divided into four chapters, including this introduction. The methods and criteria considered in the search for stationary periods are the subject of Chapter 2, whereas the results and their discussion are presented in Chapter 3. Conclusions are summarized and some suggestions for future works are left to Chapter 4. Appendices contain additional information on MATLAB scripts and a few tables.

Chapter 2

Methodology

2.1 Stationary random data

Given any physical phenomenon as a random process, it can be characterized at any time by its statistical properties over the desired period. If the statistical properties are independent of time, the random process is considered stationary, even though the random variables themselves are time-dependent. For such a process, all the statistical moments, as well as the probability density function, are independent of time (Bendat and Piersol, 2000; Kaimal and Finnigan, 1994).

This section describes the procedure used, to find periods in the Perdigão IOP measurements, where the wind flow was mostly normal to the two hills and could be considered stationary. The procedure consisted in the sequential application of filters, where the data that do not meet a certain criterion is rejected. It is expected that the time series that have successfully passed through all the filters have properties independent of time and, as such, can be considered stationary.

The filters, which were intended to check properties or perform some tests on the data, were:

1. Wind direction,
2. Integral time-scale,
3. Reverse arrangements test.

After the reverse arrangements test, three alternatives were tested to conclude the procedure:

4a. Hypothesis test,

4b. Kolmogorov–Smirnov test,

4c. Nonstationary ratio test.

As mentioned, these last tests were not applied sequentially, but alternatively. Each step of the procedure is detailed next, including its intended purpose.

2.2 Wind direction

The concern was to study wind with a direction normal to the ridges. The first criterion was based on wind direction satisfying the following parameters:

- Northeasterly winds —$45° \pm 30°$;
- Southwesterly winds —$225° \pm 30°$;
- Time intervals larger than 30 minutes.

According to Pan and Patton (2017), the maximum deviation of 30° is acceptable in this kind of surveys, to find stationary periods. The length of the intervals larger than 30 minutes is typically required to obtain adequate sampling of turbulent motions and to provide representative time-averaged statistics (Kaimal and Finnigan, 1994) and recommended in the application of the remaining statistical criteria used in this thesis.

In the end, 86 periods with southwest wind were collected in three masts (20 in trSE_04, 29 in trSE_13 and 37 in riSW_06) and 29 periods with northeast wind were collected in the mast trSE_-13.

Figure 2.1 represents a scheme of directions sought in each tower.

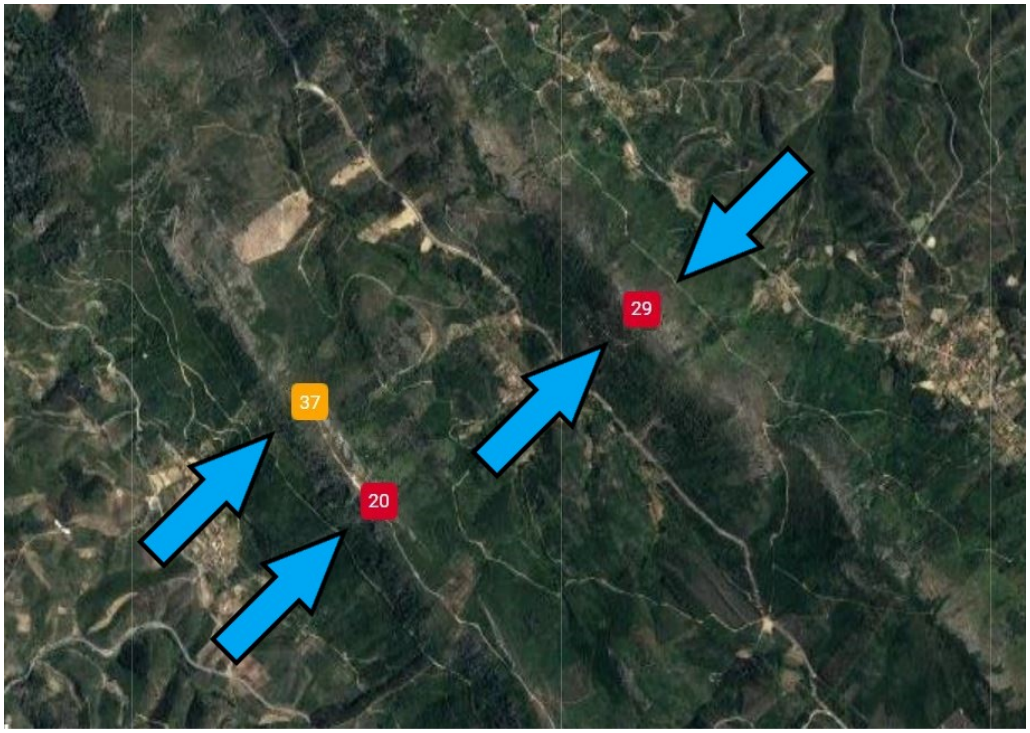

Figure 2.1: Direction winds studied

2.2.1 Reference frame rotation

One important point is the description of how the coordinate axes were chosen. To be more precise, the flow properties, such as turbulence, are anisotropic, i.e. the properties vary according to the direction in question.

In the Perdigão experiment, rectangular Cartesian coordinates were chosen, and the main concern was to align the instruments with the local direction, the z axis aligned with the geopotential gradient. For the other directions, an offset was given to be taken into account in the results.

The fluxes are measured in a local reference, which does not coincide with the equations used to analyze them.

Over complex terrain, we must be aware of them and deal with them. The approach used was to allow the flow to set the coordinate directions. The sampled velocity data are recorded in the instrument's rectangular Cartesian reference frame which denoted by u_1, v_1, w_1.

After the data had been collected, the average of each time series was calculated, to find the components of the mean wind vector (U_1, V_1, W_1). Then it was rotated, from the reference frame of the instrument to the chosen local frame according to the mean flow, using the following expressions. In this case, x was taken in the direction of the local mean wind vector u (Kaimal and Finnigan, 1994). The new velocity components are given by:

$$u_2 = u_1 \cos\theta + v_1 \sin\theta, \tag{2.1}$$

$$v_2 = -u_1 \sin\theta + v_1 \cos\theta, \tag{2.2}$$

$$w_2 = w_1, \tag{2.3}$$

where

$$\tan\theta = \frac{V_1}{U_1} \tag{2.4}$$

The remaining criteria were always applied considering the velocity in the reference frame aligned with the mean wind flow of each time series.

2.3 Integral time scale

The second criterion used to separate stationary and non-stationary random data was integral time scale below 100 s. Before defining the integral time scale it is important to understand what is the autocorrelation.

The autocorrelation function $C_\phi(\eta)$ of a variable $\phi(t)$ is a characteristic of data which shows the degree of similarity between the values of the same variables over successive time intervals (Bendat and Piersol, 2000). It is defined as the average of the product of the quantity at time t with the quantity at time $(t+\eta)$ for an appropriate averaging time T, which in this case was the length of each period. It indicates the "memory" of the phenomenon (Kaimal and Finnigan, 1994) i.e. the time over which the process is correlated with itself.

$$C_{\phi\phi}(\eta) = \langle \phi'(t) \cdot \phi'(t+\eta) \rangle \tag{2.5}$$

Here $\langle \quad \rangle$ indicates averaging over a finite duration, $\eta = t - t'$ and ϕ' is the fluctuating quantity.

$$\phi' = \phi - \langle \phi \rangle \tag{2.6}$$

The normalized version is known as autocorrelation coefficient and it is given by:

$$\rho_\phi(\eta) = \frac{C_{\phi\phi}(\eta)}{C_{\phi\phi}(0)} \tag{2.7}$$

Here $C_{\phi\phi}(0)$ is the variance of ϕ'.

The procedure is repeated for all time delays of interest. In this work, $\eta_{max} = 10\ min$ was chosen. The autocorrelation is important in this survey because it signals the presence of trends.

After introducing the autocorrelation, the second criterion used to filter stationary data, the integral time scale, becomes easier to explain.

The integral time scale measures the length of time that a variable, ϕ, is correlated with itself (Pan and Patton, 2017). It is defined by the integral of the autocorrelation coefficient shown below:

$$\tau_\phi = \int_0^\infty \frac{C_{\phi\phi}(\eta)}{C_{\phi\phi}(0)} d\eta \tag{2.8}$$

The large integral time scale indicates large eddies, a consequence of nonstationarity of the time periods found. Low integral time scale values are essentially associated with small eddies, particularly turbulence.

To estimate this parameter, there are two approaches:

1. The time lag, η, such that $C_{\phi\phi}(\eta)/C_{\phi\phi}(0) = 1/e$ is a good approximation of τ_ϕ (Kaimal and Finnigan, 1994). This is true even when the autocorrelation function is not strictly exponential and it is conceptually similar to the spectrum-based approach used by Lenschow and Stankov (1986);
2. Calculating the integral up to the first zero-crossing usually provides larger estimates of integral time scales than alternative approaches (Dias et al., 2004). This conservative approach was preferred in this work. For each time series, the integral time scale of each velocity component was calculated (τ_u, τ_v and τ_w).

2.4 Reverse arrangements test

The next criterion, the reverse arrangements test, is considered a nonparametric trend test. The main goal is to establish whether a sequence of observations (time series) include an underlying trend (Beck et al., 2006). The observations may have a wide range of probability distribution functions and this test becomes convenient where no assumption is made about it.

The reverse arrangements test appeared from the need to know, with a certain degree of confidence, if the time between repairs of an equipment was decreasing, i.e. whether the series of times between consecutive repairs had a decreasing trend (Trindade, 1995). Here it was used to verify if the average wind speed could be considered constant or, on the contrary, was increasing or decreasing

The time series which were accepted by the integral time scale criterion, were tested by this criterion, for all the three velocity components.

In this particular survey, the minimum duration of 30 minutes and the requirement of at least 10 samples for this test suggest an averaging time of $\delta t = 3$ min which fulfill $\delta t \geq 2 \times \tau_\phi$ and thus

the time series were divided into 3 min-subrecords, resulting in a sequence of N subrecords (Pan and Patton, 2017). The average over each 3 min-subrecord was determined and denoted by $\langle x_i \rangle$, $i = 1,2,3,...,N$.

The next procedure was to count the number of times that $x_i > x_j$ for $i < j$. It is called a reverse arrangement. Here, the total number of reverse arrangements is denoted by A. The general definition is:

$$h_{ij} = \begin{cases} 1 \text{ if } x_i > x_j \\ 0 \text{ otherwise} \end{cases} \tag{2.9}$$

and, finally

$$A_i = \sum_{j=i+1}^{N} h_{ij} \tag{2.10}$$

then

$$A = \sum_{i=1}^{N-1} A_i \tag{2.11}$$

Considering the sequence of N observations of the same variable is independent, then the number of reverse arrangements is a variable A, with an associated mean and variance:

$$\mu_A = \frac{N(N-1)}{4} \tag{2.12}$$

$$\sigma_A^2 = \frac{N(2N+5)(N-1)}{72} \tag{2.13}$$

In this work a level of significance $\alpha = 0,05$ was considered and the time series is considered without trend for $A_{N;1-\alpha/2} < A \leq A_{N;\alpha/2}$.

Siegal (1956) formulated another way to check whether time series has a significant trend. A Z-score can be calculated using the following equation:

$$z = \frac{A - \frac{N(N-1)}{4}}{\sqrt{\frac{2N^3+3N^2-5N}{72}}} \tag{2.14}$$

In this case, and for the same level of significance, a Z score of $z \geq 1.96$ or $z \leq -1.96$ is required to define a non-stationary time series (Bendat and Piersol, 2000).

2.5 Hypothesis test

The following criterion used in the filtering of stationary periods was the hypothesis test. The main objective was to verify whether a sample of data or their estimates were compatible with certain populations or with previously fixed parameters and the result will be one of the two possible answers. In both cases, there is a risk of giving the wrong answer. One of the characteristics of this hypothesis test is to control and minimize such risk (Guimarães and Cabral, 2011).

To facilitate the understanding of the methodology, the following steps are presented:

- Definition of hypotheses;
- Identification of the most adequate test statistic;
- Definition of the decision rule, namely the level of significance;
- Calculation of test statistics and decision making.

This study considered tests involving hypotheses related to the parameters of several samples belonging to a population (time series).

The idea was to divide the periods found into 3-min subsets and test whether they have the same averages and variances. If they did, they would become a single group and the test would proceed with the comparison of the next subset. Thus the hypotheses would be defined. The null hypothesis will be expressed by H_0:$\mu_1 - \mu_2 = 0$ and it will define the subsets which have the same average, consequently the alternative hypothesis will be expressed by H_1:$\mu_1 - \mu_2 \neq 0$ and it will represent the subsets which have not the same average.

For the case of comparison of the variances, the null hypothesis, H_0:$\frac{\sigma_1^2}{\sigma_2^2} = 1$, and it will characterize the subsets with the same variance and the alternative hypothesis, H_1: $\frac{\sigma_1^2}{\sigma_2^2} \neq 1$ and it will distinguish the subsets which do not have the same variance.

As this test use two supposedly independent samples ($\delta t \geq 2\tau_\phi$, see section 2.3) with large size because 3 min match 3240 records, the test that best fits the situation of comparing the average is the Z test and for the case of variances, the F test.

The decision to reject or not the null hypothesis is based on the value that the test statistic takes. The probability α, that in case H_0 is true the test statistic belongs to the rejection region, is designated by the level of significance of the test.

The tests used in this work always considered a level of significance of 5 %. The last step corresponds to the calculation of the test statistic and decision making. The test statistic is defined as:

$$TS = \frac{\langle X_1 \rangle - \langle X_2 \rangle - \delta_0}{\sqrt{\frac{S_1^2}{N_1} + \frac{S_2^2}{N_2}}} \tag{2.15}$$

where $\langle X_1 \rangle$ and $\langle X_2 \rangle$ represent the averages of each subset, S_1^2 and S_2^2 each sample variances and N_1 and N_2 the samples size.

For the case of comparison of the variances, the test statistic is given by:

$$TS = \frac{S_1^2}{S_2^2} \tag{2.16}$$

In agreement with what was intended, a function was written in Matlab for the calculation of the mean and in the case of variance, a function provided by the software was used.

2.6 Kolmogorov–Smirnov test

In statistics, the Kolmogorov–Smirnov test (K–S test or KS test) is a nonparametric test of the equality of continuous (or discontinuous), one-dimensional probability distributions that can be

used to compare a sample with a reference probability distribution.

The Kolmogorov–Smirnov statistic quantifies the distance between the empirical distribution function of the sample and the cumulative distribution function of the reference distribution. Here, the test was used in a different way, to compare the distribution of two samples (Smirnov, 1939).

It calls two-sample K–S test, which is one of the most useful and general nonparametric methods for comparing two samples, as it is sensitive to differences in both location and shape of the empirical cumulative distribution functions of the two samples.

The two sample Kolmogorov-Smirnov test was used to test whether two samples come from the same distribution. The procedure is very similar to the One Kolmogorov-Smirnov Test, which means that the test quantifies the distance between the empirical distribution functions of two samples, not specifying which distribution they belong to.

Suppose that the first sample has size N_1 with an observed cumulative distribution function $F(x)$ and that the second sample has size N_2 with an observed cumulative distribution function $G(x)$ (Guimarães and Cabral, 2011). Defined by:

$$D_{m,n} = max_x|F(x) - G(x)| \tag{2.17}$$

The null hypothesis was H_0: both samples come from a population with the same distribution. The test will reject the null hypothesis, at significance level $\alpha = 0,05$, if $D_{m,n} > D_{m,n,\alpha}$, where $D_{m,n,\alpha}$ is the critical value at the specified significance level. This parameter can be calculated by:

$$D_{m,n,\alpha} = c(\alpha)\sqrt{\frac{N_1 + N_2}{N_1 \cdot N_2}} \tag{2.18}$$

Here $c(\alpha)$ is the inverse of Kolmogorov distribution at α.

This test was computed using by Matlab's function. And because this test was very potent and restricted in data evaluation, 3 min-samples with lower sampling rates were used.

2.7 Nonstationary ratio

Another test used in this work was the nonstationary ratio proposed by Mahrt (1998). With this method, a time series of duration $\mathscr{T}$ is divided into I records and each record into J subrecord, each with length δt.

Being $\widetilde{\phi}_{ij}$ the average within each subrecord, the average of each record is calculated by

$$\widetilde{\widetilde{\phi}}_i = \frac{1}{J}\sum_{j=1}^{J}\widetilde{\phi}_{ij}\,, \tag{2.19}$$

where the double tilde means average over a record, i.e. over a duration $J \times \delta t$. The standard deviation of the record mean values is given by

$$\sigma_{\widetilde{\widetilde{\phi}}} = \left[\frac{1}{I-1}\sum_{i=1}^{I}\left(\widetilde{\widetilde{\phi}}_i - \widehat{\phi}^{\mathscr{T}}\right)^2\right]^{1/2}, \tag{2.20}$$

where $\widehat{\phi}^{\mathscr{T}} = 1/I\sum_{i=1}^{I}\widetilde{\widetilde{\phi}}_i$ is the mean value of the entire time series, with duration $\mathscr{T}$.

The standard deviation of the samples within each record is

$$\left(\sigma_{\approx\atop\tilde{\phi}}\right)_i = \left[\frac{1}{J-1}\sum_{j=1}^{J}\left(\tilde{\phi}_{ij} - \approx{\tilde{\phi}}_i\right)^2\right]^{1/2} . \tag{2.21}$$

The random variability of records is calculated from the average of $\left(\sigma_{\approx\atop\tilde{\phi}}\right)_i$,

$$\mathrm{RE} = \frac{\frac{1}{I}\sum_{i=1}^{I}\left(\sigma_{\approx\atop\tilde{\phi}}\right)_i}{J^{1/2}} , \tag{2.22}$$

and the nonstationarity ratio defined as

. (2.23)

It measures the ratio of the variabilities in all the time series and within records. For random samples, with $I \geq 5$ and $J \geq 5$ the variabilities should be similar and NR close to unity (Bendat and Piersol, 2000).

Mahrt (1998) proposed that a time series could be declared stationary if NR ≤ 2. In this work, despite the fact that each time series had different durations $\mathscr{T}$, $I = 5$ and $J = 6$ were always used, as in Pan and Patton (2017). This means that the length of each subrecord, $\delta t = \mathscr{T}/N$, with $N = I \times J$, changed from case to case and was not necessarily larger than the integral time scale.

Chapter 3

Results and discussion

After introducing the methodologies and their parameters used for data scrutiny, an assemblage of results and their discussion are exhibited in this chapter.

In section 3.1, the number of periods found which had wind direction perpendicular to the ridges are shown while section 3.1.1 presents the results of the discarded periods which were not considered valid for evaluation. The periods found in which their integral time scale was less than 100 seconds can be seen in the section 3.2. Section 3.3 deals with the identification of the periods which were rejected due to underlying trends through the reverse arrangements test. The results related to statistical properties and their inherent tests are shown in the following sections, such as the identification of subsets with the same average (Hypothesis test) in section 3.4, the identification of subsets with the same probabilistic distribution (K-S test) in section 3.5 and in section 3.6 the understanding of the degree to which the atmospheric flows are non-stationary.

3.1 Wind direction

The campaign domain was characterized by its double parallel ridge topography with orientation Southeast-northwest and as the main concern was to find periods in which the wind direction was perpendicular to the ridges, this led to search for time series larger than 30 minutes with orientation of $45° \pm 30°$ (NE) and $225° \pm 30°$ (SW) (section 2.2). Northeastern winds were only sought in data from tower 29 while southwestern winds were inspected in all three towers under study.

Figure 3.1 represents the number of these intervals found for each height and its respective tower. In towers 37 and 20, around 50 periods per height were found. Some exceptions are:

- small number of periods in tower 37 and 20 for height of 10 meters;
- around 100 periods in tower 20 for a height of 80 meters.

The first exception may be caused by variability of the wind direction near the surface, it was very difficult to identify periods with constant direction near the ground, with only two intervals found for heights of 10 m in each direction. The second one is due to the fact that the number is the sum of two sonic anemometers mounted at 80 m in tower 20, while every other cases are the result of only one anemometer.

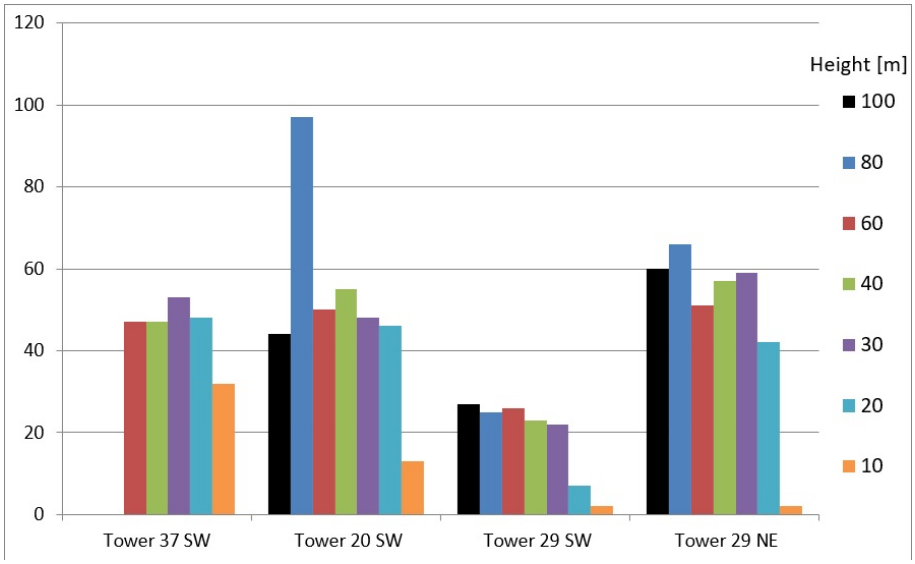

Figure 3.1: Number of periods filtered by direction

In tower 29, located in the northern ridge, winds were predominantly in the northeast direction, with around 340 periods. For the southwest direction, about 130 periods have been registered. Still, regarding this tower, periods with the intended directions close to the ground were scarse.

In conclusion, during the 45 days of the IOP, the wind was normal to the ridges in 1049 time intervals that lasted for, at least, 30 minutes.

It should be noted that some invalid periods were counted in which the anemometers were disconnected. These periods contain the last value read from the sensor, right before it turned off. Hence, these periods will be eliminated and will not be considered in the following steps.

Tables B.1–B.3, in appendix B), describe in more detail the periods found.

3.1.1 Data availability

During the IOP, there were a few days with storms, in which the anemometers were shut down. In these cases, the data logger recorded the last speed and direction values. These periods of time should be discarded. The approach used to eliminate these invalid periods is described next.

Firstly, the days with adverse climatic conditions, which could make the measurements invalid, were identified using the results of (Vilaça, 2018). Using the table 3.1, from Vilaça (2018), that describes the percentage of valid values in each day, and through a visual inspection, periods that are not valid for this study were deleted.

In total, 40 time series were deleted, since the data recorded is not valid. These eliminated periods were the following:

- **10 May**, from 15h to 16h and between 19h until 24h;
- **11 May**, from 0h to 11h and 14h until 24h;
- **12 May**, from 0h to 12h;

Days	Towers 37/rsw06	20/tse04	29/tse13
01-04 May	100	100	100
05 May	77	75	76
06-09 May	100	100	100
10 May	81	100	99
11 May	14	58	81
12 May	56	53	78
13-23 May	100	100	100
24 May	89	97	100
25 May	60	63	100
26-29 May	100	100	100
30 May	54	54	54
31 May-15 June	100	100	100

Table 3.1: Data availability [%] from Vilaça (2018).

- **24 May**, from 23h to 24h;
- **25 May**, from 0h to 9h.

The tower with less valid values was number 37. Even so, it had 209 valid periods, which were used for further analysis. In contrast, during all the IOP, tower 29 had the higher data availability. In total, 462 periods were obtained in both directions.

In the end, after the first filtering criterion, 1009 time series were considered to proceed the stationarity study. Table 3.2 expresses the number of time series that were considered for further analysis, for each tower and its respective height. Most of these periods were between 22h and 8h, when the atmosphere is usually stable. However, a few tens of periods out of these hours were also found (figure 3.2).

At this point, a period with almost 10 hours was found, but most periods last between 31 and 100 min. The duration according to the number of periods is represented in figure 3.3. Figure 3.4 shows one of the time series which were eliminated in this step, because the sonic anemometer was not working.

Height agl [m]	Towers 37/rsw06	20/tse04	29/tse13 - SW	29/tse13 - NE
100	-	42	26	60
80	-	93	24	66
60	43	48	25	51
40	43	53	22	57
30	49	46	21	59
20	45	45	6	42
10	29	11	1	2

Table 3.2: Number of valid periods for the respective tower and height.

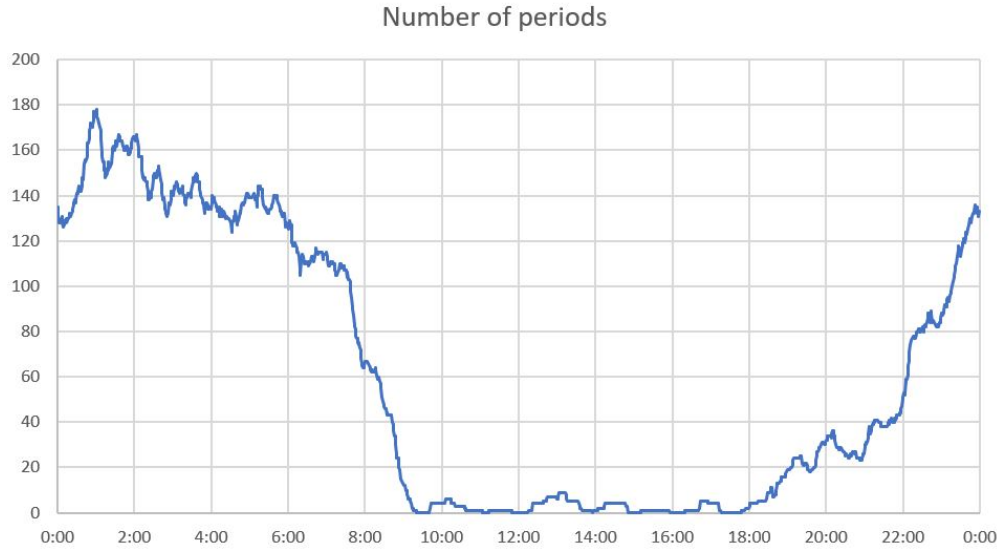

Figure 3.2: Daily time where the periods filtered by direction were found

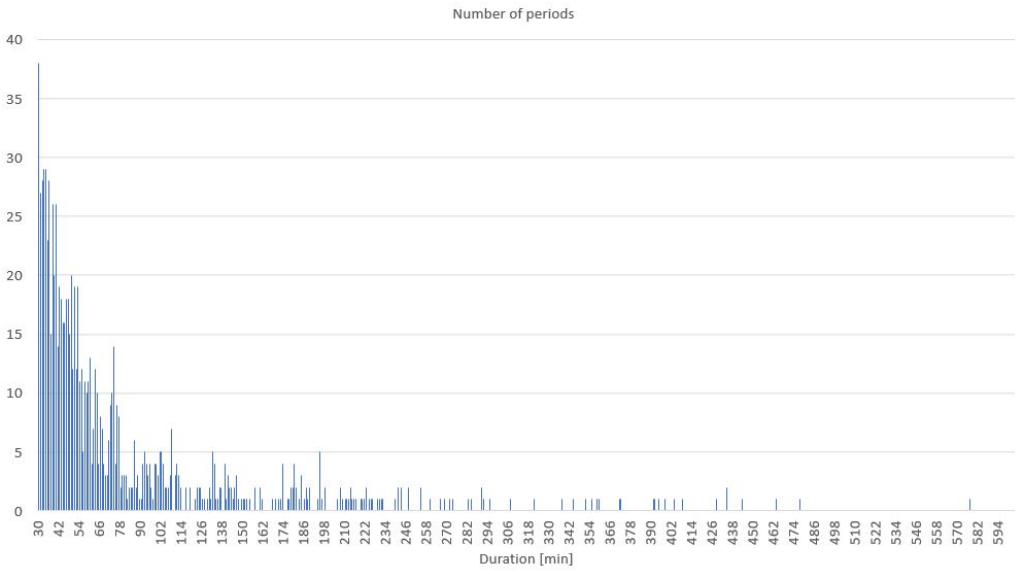

Figure 3.3: Periods characterized by its total duration after filtering direction

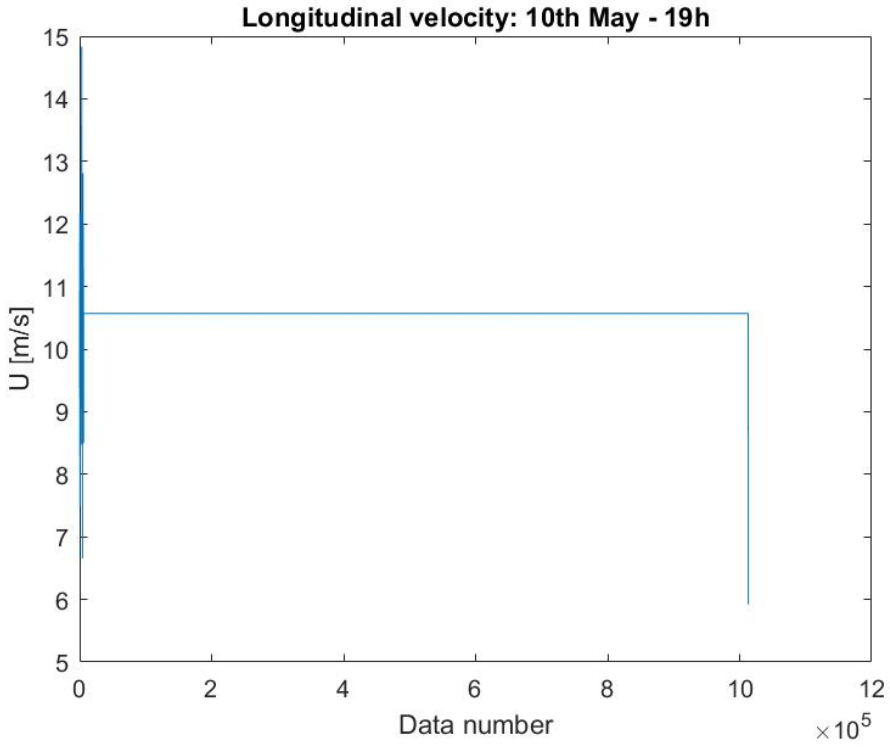

Figure 3.4: Streamwise velocity: 10 May: 19h

3.2 Integral time scale

This step tried to eliminate periods with a low-frequency variation, associated with large eddies (section 2.3). Initially, we looked for periods with integral time scale less than 90 seconds, i.e. periods in which velocity was correlated with itself for a characteristic time lower than 90 seconds. This also led to the utilization of 3 min for the length of subinterval ($\delta t \geq 2\tau_\phi$).

In the end, the limit was extended to 100 s, in order to include a few more periods. The findings are illustrated hereinafter in a certain order:

- Figure 3.5 and table C.1 describe in detail the number of intervals which satisfy the criterion for the streamwise velocity, $\tau_u \leq 100\ s$;
- Figure 3.6 and table C.2, those that comply simultaneously for the streamwise and spanwise velocity components, $\tau_{u,v} \leq 100\ s$;
- Finally, figure 3.7 and table D.3 those which fulfill simultaneously the criterion for all the three velocity components, $\tau_{u,v,w} \leq 100\ s$.

In the end, 936 time series were eliminated in this step, corresponding to about 90% of all cases. Henceforth, in total, 113 periods were studied and used in the remaining techniques. So far, the duration of the periods ranges from 30 to 87 minutes, where the majority of these periods are shorter than 50 min. May 9 and 10 appear to be the days with the most possible time intervals.

It was expected that the largest integral time scale would be in the flow direction and the lowest in the vertical direction. In the end, this was confirmed: the average integral scale of the streamwise

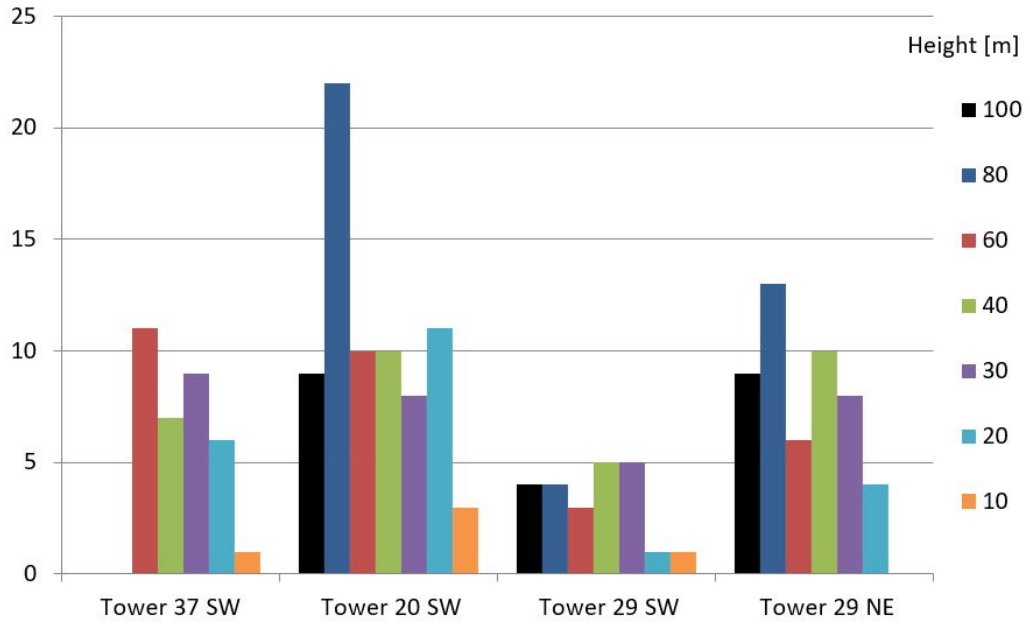

Figure 3.5: Periods with $\tau_u \leq 100$ seconds

velocity was about 53 seconds, 45 seconds for the spanwise velocity and 19 seconds for the vertical velocity.

Also, for these periods, the autocorrelation function of the variance was calculated, using the same technique explained in section 2.3. Values for for the streamwise velocity between 2.3 and 63.1 s were obtained, with an average of about 16 s. This means that the integral time scale of the variance was typically smaller than that calculated of the average. Thus, it can be concluded that $\delta t = 3$ min provides approximately independent samples, being appropriate to estimate both the average and the variance.

Two autocorrelation plot examples, in random time, can been see in figures 3.8 and 3.9. Acording to Pan and Patton (2017), the integral time scale lower than 100 s is a proper value to filter effects of the large scales, which seems to be confirmed by a visual inspection of velocity plots. Figure 3.10 shows a time series in which it is possible to observe the overlapping of a signal of high-frequency, turbulence, with another one of lower frequency, associated with large eddies and nonstationarity. The integral time scale higher than 100 seconds dictated that this series was classified as non-stationary. For comparison, figure 3.11 presents a time series where the low-frequency component is absent. Figures 3.10, 3.11 are examples of streamwise velocity where the second figure looks more stationary than the first one. The figure 3.11 has the integral time scale below 100 s and it is one of the examples that was accepted by the criterion.

For comparison of which kind of intervals were excluded in this criterion, it is presented in figure 3.12, the temporal location of the periods which were accepted and figure 3.13 that expresses that duration. Comparing figure 3.2 and 3.12, it is clear that this criterion eliminated periods during the entire day and not only confined the elimination of periods atnspecific hours. Interestingly though, this criterion eliminated all periods larger than 90 minutes.

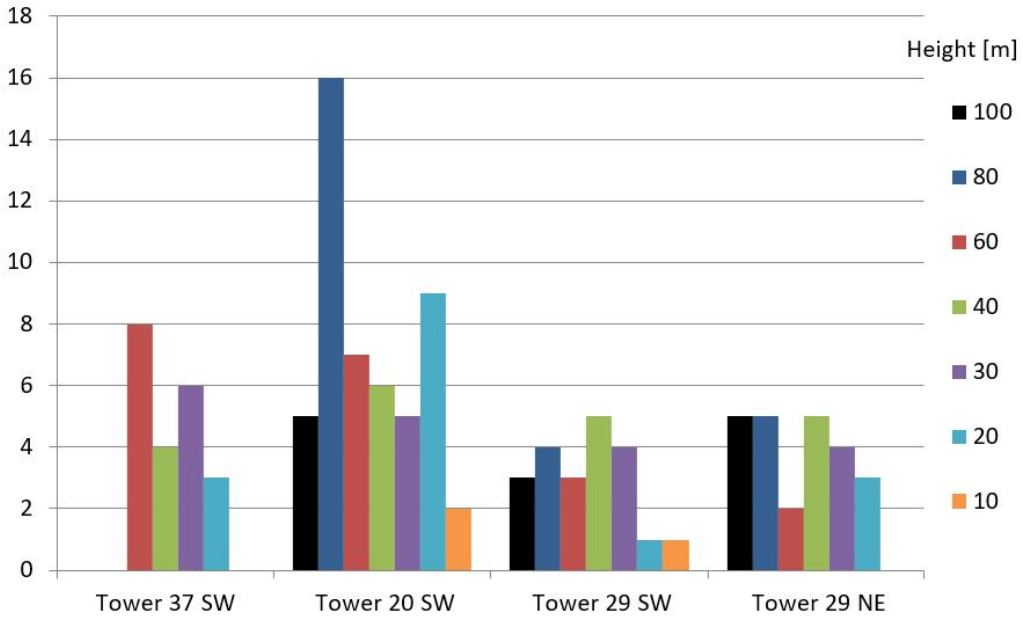

Figure 3.6: Periods with $\tau_v \leq 100$ seconds

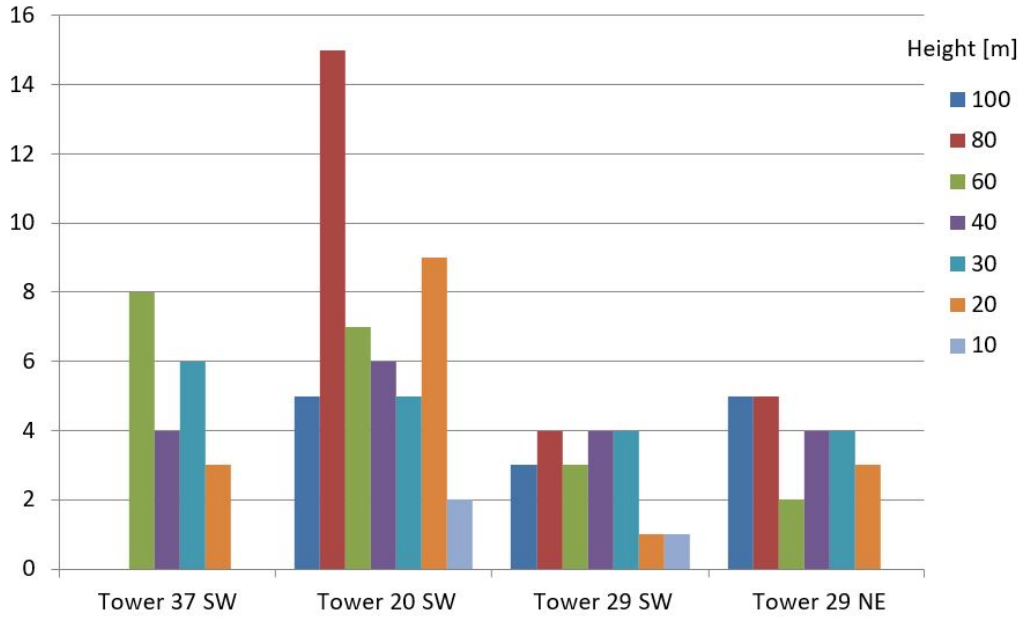

Figure 3.7: Periods with $\tau_w \leq 100$ seconds

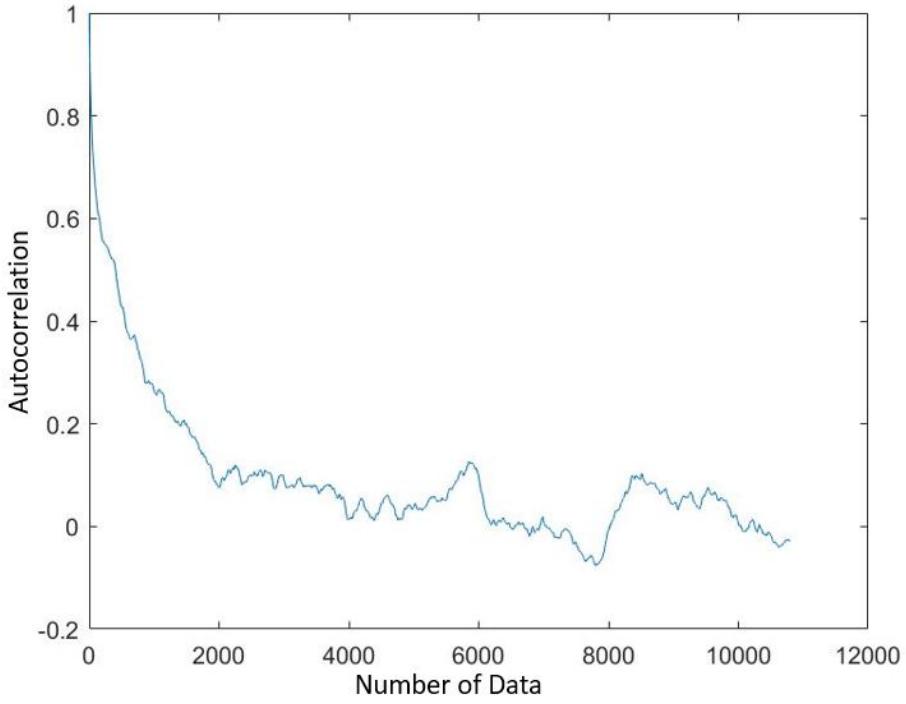

Figure 3.8: Autocorrelation plot in tower 20 at 20 m

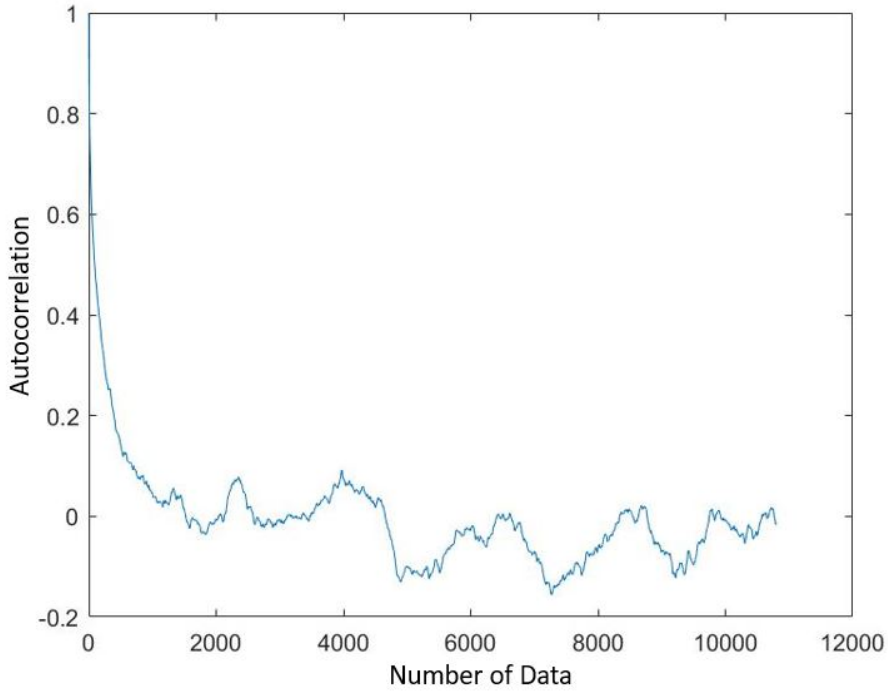

Figure 3.9: Autocorrelation plot in tower 20 at 10 m

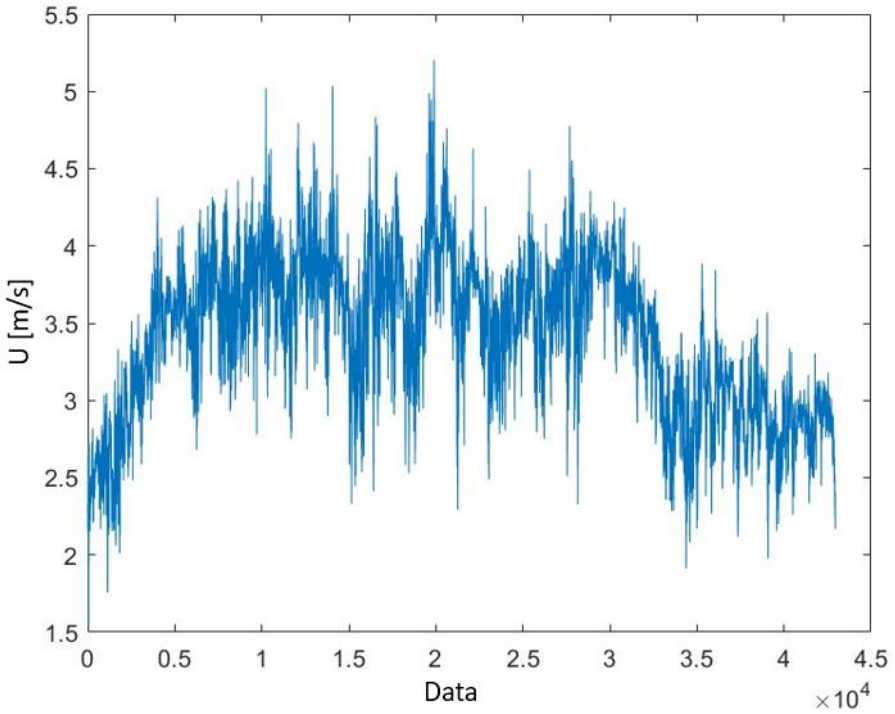

Figure 3.10: Streamwise velocity in tower 20 at 10 m with $\tau_u = 135\ s$

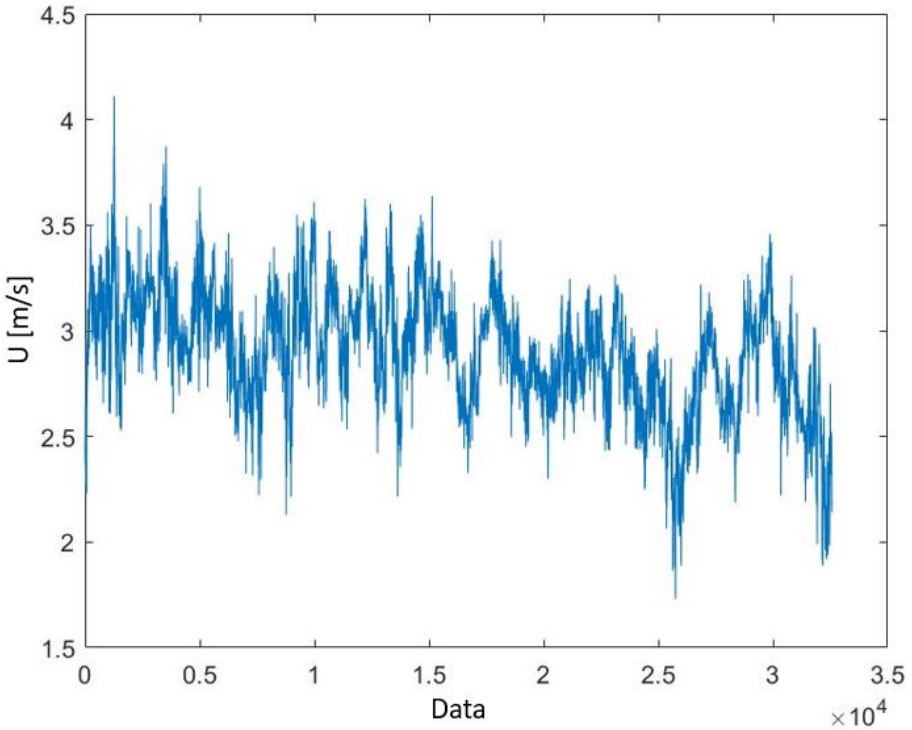

Figure 3.11: Streamwise velocity in tower 20 at 20 m with $\tau_u = 96\ s$

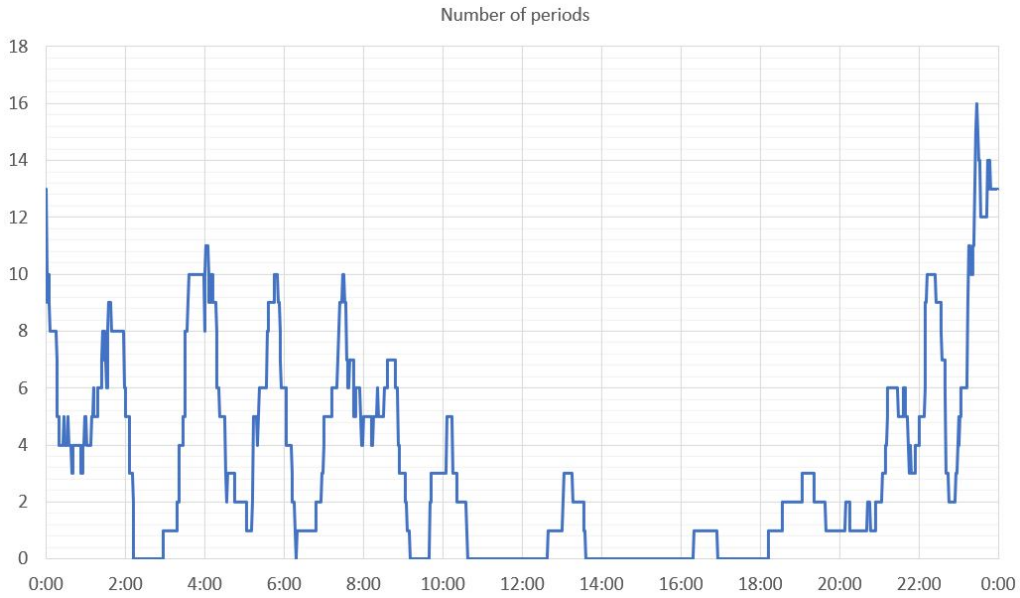

Figure 3.12: Daily time where the periods filtered by direction were found after the integral time scale criterion.

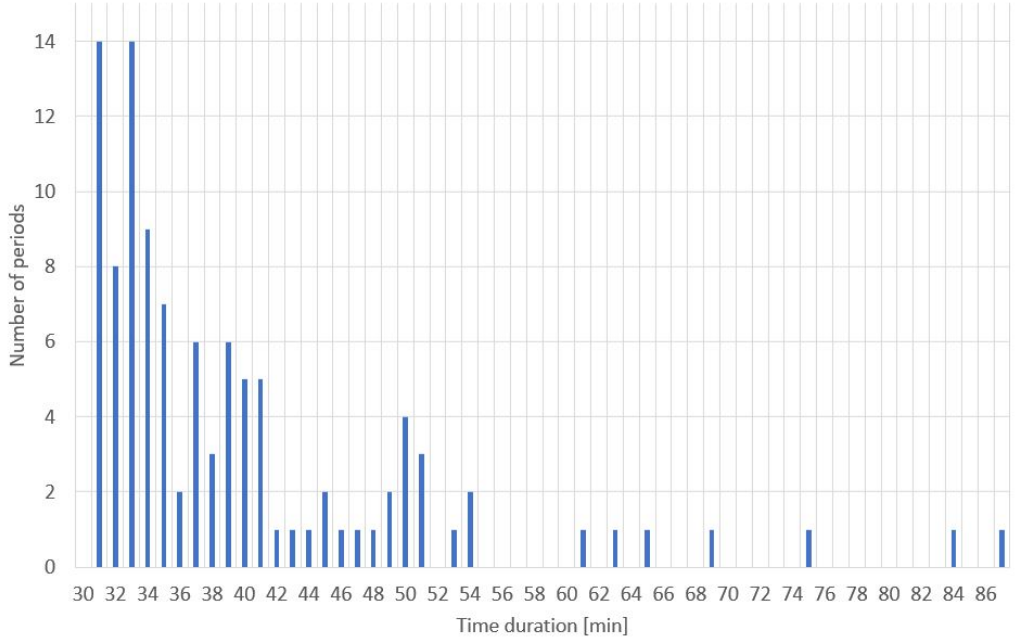

Figure 3.13: Periods characterized by its total duration after the integral time scale criterion.

3.3 Reverse arrangements test

The reverse arrangement test is selected as the basic statistical operation to construct an approach that determines both the occurrence and the duration of stationary periods. This test only measures mean trends. The probabilities for a time series of velocity components to show positive and negative mean trends are approximately equal and its range is greater than other common tests, (Pan and Patton, 2017), and therefore the reverse arrangement test is more desirable and provides finer stationary measures. The minimum duration of 30 min and the requirement of at least 10 samples for the reverse arrangements test suggest an averaging time of $\delta t \geq 3\ min$, which satisfies $\delta \geq 2 \times \tau_u$.

Hereafter, stationarity of average velocity is evaluated by applying the reverse arrangement test to time series of 3-min averaged samples, this in the three velocity components.

This approach, mentioned in section 2.4, allowed to locate nonstationary subperiods at the significance level, $\alpha = 5\ \%$, within each period, N_{total} records. Given the start point and the end point, the concerned subintervals were removed so as to form longer periods with the remainders because of a time period may contain several stationary subperiods separated by nonstationary subperiods, thus the analysis consisted of two steps:

- Determining whether the entire time series passes the test;
- Within the time series, locate the subperiods that pass the test and remove the remaining samples, since they are non-stationary subperiods.

Figure 3.14 and table D.1 describe the results obtained, that is the number of time series considered stationary according to the exposed criterion.

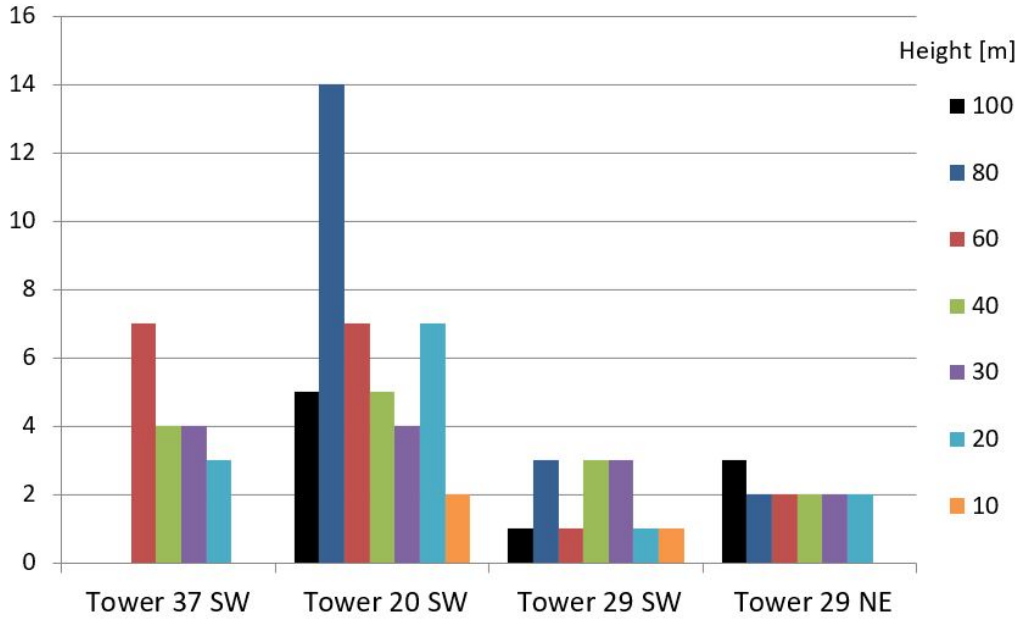

Figure 3.14: Periods which were accepted by the reverse arrangements test for the streamwise velocity

Time intervals				
Designation	**After step 2**		**After step 3**	
	Duration [s]	τ_u **[s]**	**Duration [s]**	τ_u **[s]**
Twr37_20m_May 13	2650	88,05	2000 ($\approx$ 33 min)	18,21
Twr37_40m_May 10	2965	93,52	2600 ($\approx$ 43 min)	32,89
Twr20_40m_May 11	2980	50,68	2400 (= 40 min)	27,70
Twr20_60m_May 11	3173	91,40	2400 (= 44 min)	40,64
Twr20_60m_May 29	2894	20,48	2000 ($\approx$ 33 min)	21,22
Twr20_60m_May 11	3010	53,72	2400 (= 40 min)	22,85
Twr20_100m_May 10	2724	9,79	2200 ($\approx$ 37 min)	23,41
Twr29_40m_NE_May 20	2652	74,99	2400 (= 40 min)	81,84
Twr29_60m_NE_May 23	3016	9,44	2200 ($\approx$ 37 min)	19,26

Table 3.3: Changes on integral time scale and on total duration. Step 2 means the integral time scale criterion, while step 3 is related to the procedure to eliminate non-stationary subperiods.

It needs to be emphasized that 9 periods were found that were not accepted by the criterion. However, the non-stationary subperiods were located and consequently were eliminated, outlasting only stationary subperiods.

Thus, the time series became shorter. This led to some changes in the total duration and the integral time scale at streamwise component, which are shown in table 3.3.

After that, using the remaining time periods so far, it was checked whether the time series still passed in the test, but in this case with the spanwise and vertical velocity components.

Primarily, the accepted periods of the spanwise component are presented in figure 3.15 and table D.2. Lastly, the final results, which fulfill the criterion in all velocity components, are listed in figure 3.16 and table D.3.

From 113 periods obtained in the previous criterion, the reverse arrangements test allowed to get 58 periods which were considered stationary.

In order to realize which intervals were accepted or rejected by this test, at least in a visual shape, the following figures were given representing some examples of the various periods studied.

Figure 3.17 represents a time series which was accepted, while the time series in figure 3.18 was not. Apparently, the rejected time series rejected appeared does not have any trend, however, it does. That is why the reverse arrangements test is so important, it can detect a underlying trend.

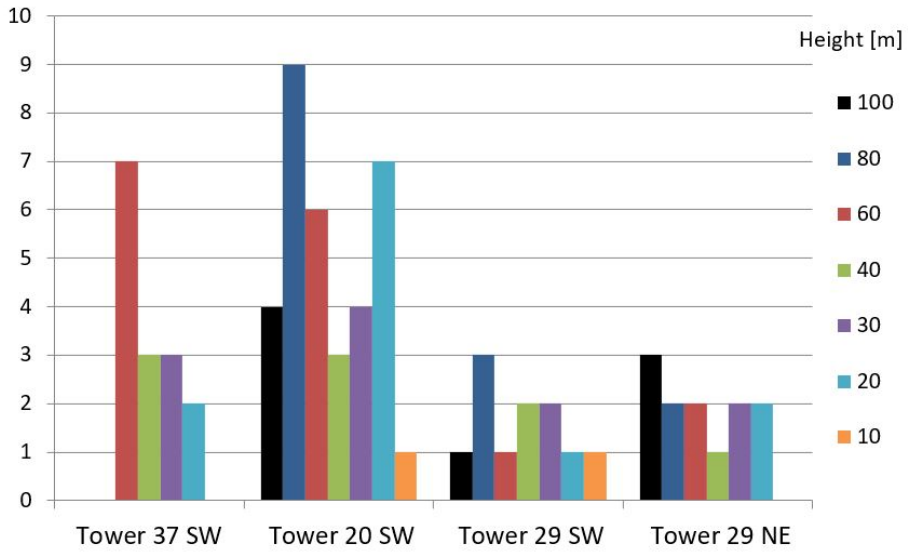

Figure 3.15: Periods which were accepted by reverse arrangements test in spanwise velocity

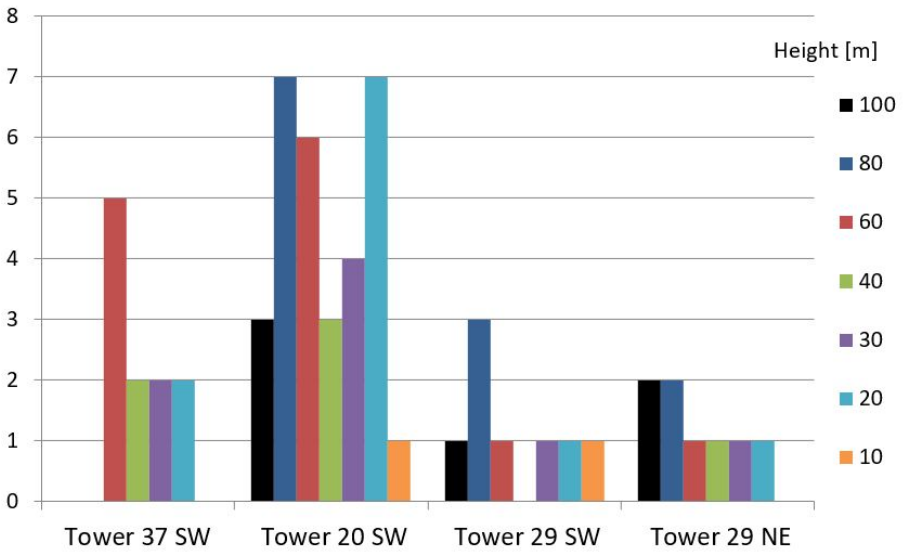

Figure 3.16: Periods which were accepted by reverse arrangements test in all of three velocity components

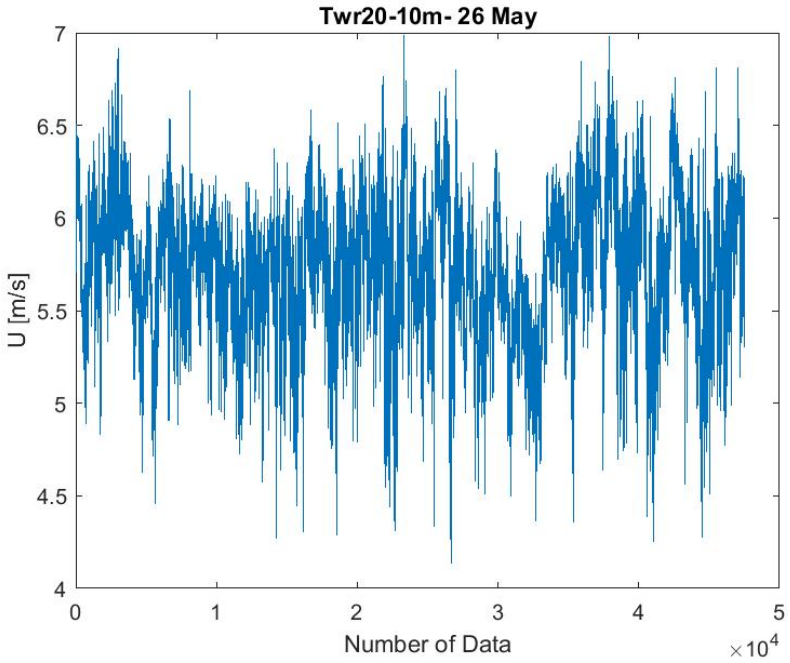

Figure 3.17: Streamwise velocity in tower 20 at 10 meters, southwestern wind, accepted after reverse arrangements test.

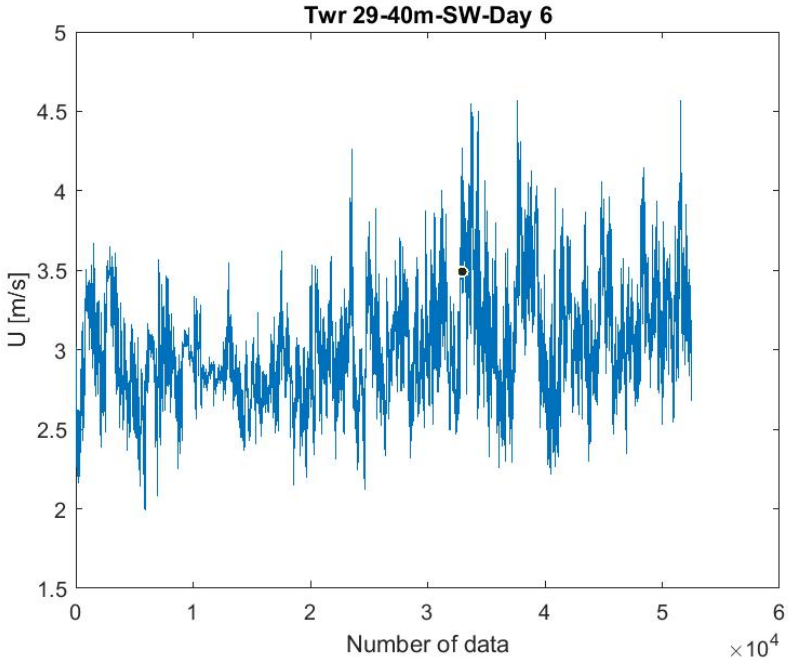

Figure 3.18: Streamwise velocity in tower 29 at 40 meters, southwestern wind, rejected after reverse arrangements test.

3.3.1 Sensitivity analysis

This section discusses the sensitivity of the criterion to the sample size and the need to understand why some time series are rejected by the reverse arrangements test.

Extending the sample size to 6 minutes means that each subinterval will be at least 4 times larger than the integral time scale. Therefore, it is expected that there will be less variability between subintervals and, consequently, the number of periods which are accepted by the criterion would be larger.

Thus, the same criterion with 6 min subsets was applied to periods that were reject when 3 min subsets were considered. That evaluation was done for all three velocity components.

In total, 113 periods were submitted for streamwise velocity by the reverse arrangements test at $\delta t = 3$ min and remaining 25 rejected periods. Taking those periods the test was repeated although using subintervals of 6 min. Table 3.4 represents the results. Other reasons can be assigned as a cause of rejection of some periods.

As mentioned before, every subperiod contains 3240 data which leads to an inaccurate evaluation because not all data is taken into account. The starting point in the first subset of the period under analysis is considered a key factor to calculate the period average since it affects its value. This could be avoided if each point of the period was evaluated in particular in order to understand which database better describe the total time series.

Reverse arrangement test		**Streamwise velocity**	**Spanwise velocity**		**Vertical velocity**	
#N°	**Designation**	6 *min* **streamwise**	3 *min* **spanwise**	6 *min* **spanwise**	3 *min* **vertical**	6 *min* **vertical**
1	Twr20-20m: May 13	X	X	X	X	X
2	Twr20-20m: June 8	-	X	X	X	X
3	Twr20-30m: June 14	X	X	X	X	X
4	Twr37-30m: May 10	-	X	X	-	-
5	Twr37-30m: May 12	X	-	X	-	-
6	Twr20-40m: May 29	X	X	X	X	X
7	Twr37-60m: May 26	-	X	X	-	-
8	Twr29-100m-NE: May 7	X	-	-	X	X
9	Twr29-100m-NE: May 20	-	X	X	-	-
10	Twr29-100m-SW: May 6	X	-	X	X	X
11	Twr29-100m-SW: May 26	X	X	X	X	-
12	Twr29-20m-NE: May 24	-	X	X	-	X
13	Twr29-30m-NE: June 8	X	X	X	X	X
14	Twr29-30m-NE: May 20	X	-	X	X	X
15	Twr29-30m-SW: May 22	X	X	X	-	-
16	Twr29-40m-NE: June 1	X	-	-	X	X
17	Twr29-40m-NE: May 15	X	X	X	X	X
18	Twr29-40m-SW: May 6	-	-	-	X	X
19	Twr29-60m-SW: May 6	-	-	-	X	X
20	Twr29-60m-SW: June 14	-	X	X	-	X
21	Twr20-80mSE: May 11	-	X	X	X	X
22	Twr29-80m-NE: May 23	-	-	X	-	-
23	Twr29-80m-NE: May 23	X	X	-	-	-
24	Twr29-80m-NE: May 23	-	-	-	X	X
25	Twr29-80m-SW: June 14	-	-	-	-	-

Table 3.4: Exceptions periods which were accepted by the reverse arrangements test for the streamwise velocity, 6 min subset

In the end, 7 more periods were considered acceptable and plausibly stationary because they

passed the criterion in all velocity components for 6 min subintervals.

It means that, for the following statistical techniques, 65 periods were considered, corresponding to about 6% of the data previously accepted by the direction criterion. Tower 20 at 20 m was the point where the highest number of periods was found.

To be more precise, 11 periods were found in tower 37 and 34 periods in tower 20. Finally, in tower 29, for the case of southwestern wind, 11 periods were considered and, for the case of northeastern wind, 65 periods in total.

3.4 Hypothesis test

As mentioned in section 2.5, in the time series for the streamwise velocity, each period was divided into 3-min subsets and consecutive subsets were tested, to check if it could be considered that they were subsets of a large set with the same average, at 95% of confidence, those subsets were gathered to reach the longest subsets' groups.

This approach used entire records inside of each subset i.e. 3240 records were used to average the subset. Through the results in table 3.5, the longest possible group of subset had 6 minutes, in the total 27 subsets. With these results, it is concluded that, within each 3 min interval, the samples are not actually independent, since the interval between two samples is much smaller than the integral time scale.

Therefore, the test results in a very narrow confidence interval for the average, because the size of the interval is inversely proportional to the size of the sample.

Consequently, the test becomes very demanding and restricted and it is difficult for two consecutive intervals to be compatible with what it is looking for. Since there are no tests for samples that are not independent, the solution is to increase the time between two consecutive samples. In the threshold, one can reach the value of the integral time scale.

Hypothesis test-Number of 6-min subset

Height agl [m]	**Tower 37**	**Tower 20**	**Tower29**	
Direction	Southwest	Southwest	Southwest	Northeast
100	-	0	3	1
80	-	6	0	0
60	4	3	0	0
40	2	2	0	0
30	1	0	1	1
20	1	1	0	1
10	0	1	0	0

Table 3.5: Number of 6 min subset found with the same average in streamwise velocity

The extensive amounts of groups of subset led to use another way to average the subset. Thus, the new approach was to pick a few records to describe the average of each subinterval.

One alternative is to use data with lower sample rates, of 3 Hz, 1 Hz and 1/3 Hz. With this approach, the test reached many subsets which were over than 6 minutes duration. Table 3.6

represents the number of reached subset while figure 3.19 schematizes the number of substets per tower and per height.

Hypothesis test-Number of subset $\geq$ 6 min				
Height agl [m]	**Tower 37**	**Tower 20**	**Tower29**	
Sample Rate	Southwest	Southwest	Southwest	Northeast
18 Hz	8	14	4	4
3 Hz	17	42	7	12
1 Hz	24	61	13	17
1/3 HZ	84	84	20	22

Table 3.6: Number of subset $\geq$ 6 min found with the same average at different sample rates

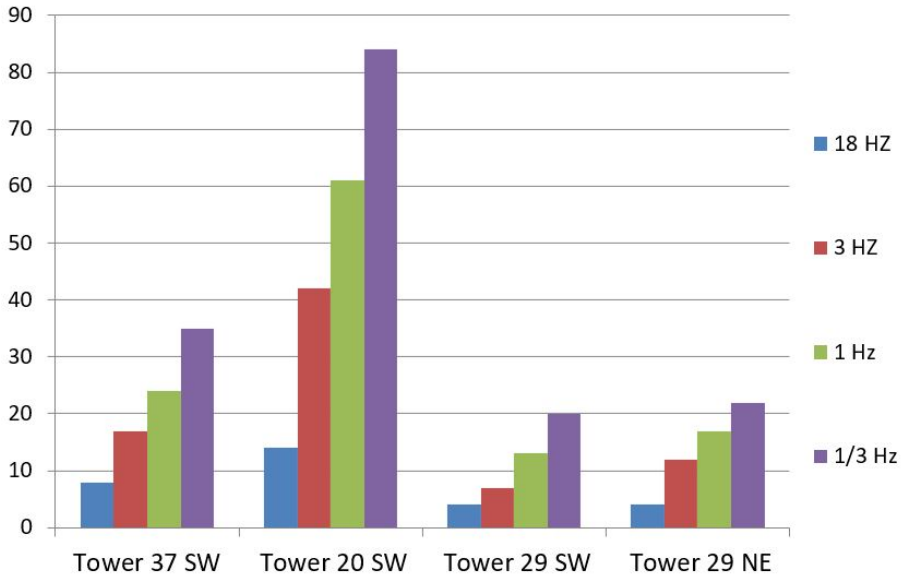

Figure 3.19: Number of subset $\geq$ 6 min found with the same average at different sample rates

At this stage, the duration of each time interval is described, function of the sample rate considered. Using the entire data of each period i.e. using 18 Hz as the sample rate, it only was possible to form periods of 6 minutes.

However, with lower sample rates, periods up to 24 minutes were found. Comparing the results obtained with 18 Hz and 1/3 Hz, there was an increase of 18% in the number of periods in tower 37, a 13% increase in tower 20 and a 12% increase in tower 29. The sizes of periods for each sample rate are listed:

- for 3 Hz: periods between 6 and 12 minutes;
- for 1 Hz: periods between 6 and 18 minutes;
- for 1/3 Hz: periods between 6 and 24 minutes;

Table 3.7 describes in which tower at 3 Hz, the various duration of the subperiods were found. Table 3.8 and 3.9 describe for 1 Hz and 1/3 Hz, respectively.

Hypothesis test-Number of subset with different duration, at 3 Hz

Duration's subset [min]	**Tower 37**	**Tower 20**	**Tower29**	
Direction	Southwest	Southwest	Southwest	Northeast
6	17	36	7	9
9	0	6	0	2
12	0	0	0	1

Table 3.7: Number of subset with different duration at 3 Hz

Hypothesis test-Number of subset with different duration, at 1 Hz

Duration's subset [min]	**Tower 37**	**Tower 20**	**Tower29**	
Direction	Southwest	Southwest	Southwest	Northeast
6	20	46	13	11
9	4	11	0	4
12	0	3	0	1
15	0	0	0	1
18	0	1	0	0

Table 3.8: Number of subset with different duration at 1Hz

Hypothesis test-Number of subset with different duration, at 1/3 Hz

Duration's subset [min]	**Tower 37**	**Tower 20**	**Tower29**	
Direction	Southwest	Southwest	Southwest	Northeast
6	24	49	13	10
9	10	23	5	8
12	1	5	2	2
15	0	2	0	1
18	0	5	0	0
24	0	0	0	1

Table 3.9: Number of subset with different duration at 1/3 Hz

Hypothesis test - SW wind						
Date	**Tower**	**Height**	**18 Hz**	**3 Hz**	**1 Hz**	**1/3 Hz**
	20	60	0	0	1×6min	2×9min
	20	60	2×6min	1×6min 1×9min	2×9min	1×24min
4 May	20	100	0	1×6min	1×6min	2×6min
	20	80 NW	1×6min	1×6min	1×6min; 1×9min	1×9min; 1×12min
	20	80 SE	2×6min	2×6min	2×6min	3×6min; 1×9min
	37	30	0	1×6min	1×9min	1×9min
	29	100	0	1×6min	1×6min	1×6min
	29	100	1×6min	2×6min	2×6min	4×6min; 2×9min; 1×12min
6 May	29	30	0	1×6min	2×6min	2×6min
	29	80	1×6min	1×6min	1×6min; 1×9min	2×6min; 1×12min
	29	80	0	0	0	2×6min; 1×9min
	20	20	0	0	0	1×6min
	20	40	0	1×6min	1×6min	2×6min
	20	60	0	1×9min	1×9min	1×6min; 2×9min
9 May	37	40	3×6min	4×6min	3×6min; 1×12min	3×6min; 1×9min; 2×12min
	37	60	0	0	0	1×6min
	37	60	0	1×6min	1×6min	1×6min; 1×12min
	37	60	0	1×6min	2×6min	1×6min; 1×9min
	20	30	1×6min	2×6min	2×6min	1×6min; 1×9min; 1×12min
	20	40	1×6min	1×9min	1×9min; 1×12min	1×9min; 1×12min
10 May	20	60	0	1×6min	2×6min	4×6min
	20	100	0	0	1×6min	1×6min
	20	80 SE	1×6min	2×6min	3×6min	4×6min; 1×9min
	37	20	0	2×6min	3×6min	5×6min
	37	60	0	1×9min	1×9min	1×9min
11 May	20	60	1×6min	2×6min	2×6min; 1×9min	1×6min; 2×9min
	20	80 SE	0	1×6min	1×6min; 2×9min	1×6min; 2×9min

Hypothesis test - SW wind						
Date	**Tower**	**Height**	**18 Hz**	**3 Hz**	**1 Hz**	**1/3 Hz**
12 May	20	80 NW	1×6min	3×6min	3×6min; 1×9min	2×6min; 1×9min; 1×18min
13 May	20	20	0	0	0	1×6min
	20	20	1×6min	1×6min; 1×9min	1×6min; 1×9min	1×18min
	20	30	0	1×6min	1×6min	2×6min; 1×9min
	20	30	0	2×6min	3×6min	1×6min; 2×9min
	20	100	0	0	2×6min	2×6min
	20	80 NW	1×6min	2×6min	3×6min	2×9min
	29	10	0	0	1×6min	1×6min
	37	20	0	2×6min	1×6min; 1×9min	2×9min
25 May	20	20	0	0	0	2×6min; 1×9min
26 May	20	10	1×6min	2×6min	1×9min; 1×15min	1×6min; 1×9min; 1×15min
	20	20	0	0	0	1×6min
	20	80 SE	1×6min	1×6min	1×6min; 1×9min	2×6min; 1×9min
	29	20	2×6min	2×6min	3×6min	3×6min; 1×12min
	29	80	0	1×6min	2×6min	2×6min
	37	30	0	0	1×6min	2×6min
27 May	20	20	0	2×6min	1×6min; 1×12min; 1×18min	3×6min; 1×18min
28 May	37	40	2×6min	2×6min; 1×9min	3×6min; 1×9min	1×6min; 1×9min; 1×15min
	37	60	0	0	0	0
29 May	20	20	0	1×6min	1×6min	1×9min
	20	30	0	1×6min	4×6min	1×6min; 2×18min
	20	40	1×6min	1×6min	2×6min	3×6min
	20	40	0	2×6min	2×6min	4×6min
	20	60	1×6min	3×6min	3×6min	2×6min; 1×9min

Hypothesis test - SW wind						
Date	**Tower**	**Height**	**18 Hz**	**3 Hz**	**1 Hz**	**1/3 Hz**
2 June	20	20	1×6min	1×9min	1×6min; 1×9min	2×6min; 1×9min; 1×15min
14 June	20	30	0	2×6min	2×6min	2×6min; 1×9min
	29	60	1×6min	2×6min	3×6min	1×6min; 1×9min

Table 3.10: Results of hypothesis test for each period, at all sample rate used, SW wind

Hypothesis test - NE wind						
Date	**Tower**	**Height**	**18 Hz**	**3 Hz**	**1 Hz**	**1/3 Hz**
3 May	29	30	0	0	0	0
15 May	29	30	1×6min	1×6min	1×6min	2×6min
20 May	29	40	0	2×6min; 1×9min	2×6min; 1×9min	2×6min; 2×9min
23 May	29	60	1×6min	1×6min	2×6min	1×9min; 1×12min
	29	80	0	0	0	1×9min
	29	100	0	2×6min	2×6min	2×6min; 1×9min
24 May	29	20	0	0	3×6min	2×6min; 1×9min
7 June	29	80	0	0	1×6min	1×6min; 1×9min
8 June	29	30	1×6min	2×6min	3×6min	2×6min; 2×9min
	29	100	0	0	0	1×6min
10 June	29	40	0	1×12min	1×12min	1×24min

Table 3.11: Results of hypothesis test for each period, at all sample rate used, NE wind

Thereafter, spanwise and vertical components were analysed. As in streamwise component, the periods obtained were equally hard to get and they did not larger more than 9 minutes. Consequently, similar to the approach taken for the streamwise component, the results for the remaining components were obtained for lower values of the sample rate. Here, tables x and y present the results at 1/3 Hz.

Hypothesis test - SW wind				
Date	**Tower**	**Height**	**V**	**W**
4 May	37	30	1x6min; 1x9min	1x6min; 1x9min
	20	60	4x6min	1x6min; 1x12min
	20	60	2x6min	1x6min; 1x9min; 1x15min
	20	100	2x6min	1x6min; 1x9min; 1x12min
	20	80 NW	3x6min; 1x9min	2x6min; 1x18min
	20	80 SE	1x6min	2x6min; 2x9min
6 May	29	100	4x6min	2x6min; 1x9min; 1x15min
	29	100	2x9min	2x6min; 2x12min
	29	30	1x12min; 1x18min	3x6min; 1x9min
	29	80	2x6min; 2x9min; 1x15min	1x6min; 2x9min; 1x15min
	29	80	3x6min; 1x9min	1x6min; 1x15min
9 May	20	20	1x6min	1x6min; 1x9min; 1x12min
	37	40	1x6min	1x6min; 1x15min; 1x21min
	37	60	3x6min	1x6min; 2x9min

Hypothesis test - SW wind				
Date	**Tower**	**Height**	**V**	**W**
9 May	20	40	2x6min; 1x15min	1x6min; 1x12min
	37	60	3x6min	1x6min; 1x12min; 1x18min
	20	60	3x6min; 1x9min	1x6min; 1x9min; 1x15min
	37	60	4x6min; 1x9min	2x6min; 1x9min; 1x15min
10 May	37	20	1x9min; 1x18min	1x6min; 1x18min
	20	30	3x6min	2x9min; 1x12min
	20	40	2x6min	1x12min; 1x18min
	20	60	3x6min; 2x9min	2x6min; 1x9min; 1x12min; 1x18min
	20	100	1x6min; 1x15min	1x27min
	37	60	3x6min	2x9min; 1x12min; 1x15min
	20	80 SE	2x6min; 1x9min; 1x12min	1x9min; 1x12min; 1x15min; 1x24min
11 May	20	60	3x6min; 2x9min	2x6min; 1x27min
	20	80 SE	2x6min; 1x9min; 1x21min	1x36min
12 May	20	80 NW	2x9min; 1x15min	1x9min; 1x18min

Hypothesis test - SW wind				
Date	**Tower**	**Height**	**V**	**W**
13 May	29	10	1x9min; 1x12min	1x9min; 1x21min
	20	20	2x6min; 1x9min	2x6min; 1x9min
	20	20	3x9min	3x6min; 1x9min
	37	20	2x6min	2x6min; 4x9min
	20	30	4x6min	2x6min; 1x12min; 1x18min
	20	30	1x12min; 1x15min	1x6min; 1x9min; 1x15min
	20	100	2x6min; 1x9min	2x6min
	20	80 NW	1x6min	1x6min; 1x9min; 1x12min
25 May	20	20	2x6min	2x6min
26 May	20	10	4x9min	1x6min; 1x36min
	29	20	1x6min	2x6min; 1x12min
	20	20	1x6min; 3x9min	1x6min; 1x30min
	37	30	3x6min	1x6min; 1x9min
	29	80	3x6min	1x6min; 1x9min
	20	80 SE	3x6min; 1x9min	3x6min; 1x9min
27 May	20	20	2x6min	3x6min; 1x9min; 1x12min

Hypothesis test - SW wind				
Date	**Tower**	**Height**	**V**	**W**
28 May	37	40	3x6min; 1x12min	1x6min; 1x9min; 1x12min; 1x15min
	37	60	1x6min; 1x9min	1x6min; 2x9min
29 May	20	20	3x6min	3x6min; 1x12min
	20	30	1x6min	3x6min; 1x9min
	20	40	1x6min	1x6min; 1x12min; 1x18min
	20	40	1x6min; 2x9min	3x6min; 2x9min
	20	60	4x6min; 1x9min	3x6min
2 June	20	20	1x9min	1x6min; 1x9min
14 June	30	20	1x6min; 1x9min; 1x12min	3x6min; 1x9min; 1x12min
	29	60	3x6min; 1x9min; 1x12min	2x9min; 1x12min

Table 3.12: Results of hypothesis test for each period for spanwise and vertical components, at 1/3 Hz, SW wind.

Hypothesis test - NE wind				
Date	**Tower**	**Height**	**V**	**W**
3 May	29	30	2x6min; 1x9min	2x6min
15 May	29	40	0	1x6min; 2x9min
20 May	29	30	1x6min; 1x9min	3x6min; 1x9min
23 May	29	100	1x6min; 1x9min; 1x15min	2x6min; 2x9min
	29	60	1x9min; 1x15min	1x6min; 2x9min; 1x15min
	29	80	3x9min; 2x12min; 1x18min	1x6min; 1x9min; 1x24min
24 May	29	20	1x6min	1x9min; 2x12min
7 June	29	80	0	2x6min; 1x12min
8 June	29	100	4x6min; 1x9min	3x6min
	29	30	3x6min; 1x9min	1x6min; 1x9min; 1x12min
10 June	29	40	1x6min	2x6min; 1x9min; 1x12min

Table 3.13: Results of hypothesis test for each period for spanwise and vertical components, at 1/3 Hz, NE wind.

3.5 Kolmogorov–Smirnov test

The goal of this test was verifying if the data from consecutive 3 min periods could be considered has belonging to the same statistical distribution. It is more complete than the hypothesis test for the average, since data belonging to the same distribution will have identical statistical moments of any order, not only the first. This test used also a confidence interval of 95%.

Initially, 65 periods were tested using the raw data, i.e. a sample rate of 18 Hz, however similarly to the hypothesis test, it was not possible to find any consecutive periods which could be considered from the same distribution. This happened also because the samples are not necessarily independent. As solution, it was decided to extend the test decreasing the sample rate.

Subsets with sample rate 1/3 Hz were considered for the three velocity components. Tower 20 was the location where almost all the subsets with the same distribution were found. This is expected, since there was the place where most periods passed the reverse arrangements test.

For the streamwise velocity, the longest group found was about 24 minutes, and about 20 periods of 9 min and 6 periods of 15 min were found. In the spanwise component, the size of the longest period decreased, comparing with the streamwise velocity, however, it was of 21 minutes. In this case, around 30 9 min periods were found, more than in the streamwise velocity. Finally, in the vertical component, inside a time series of 48 minutes, a period with the same distribution lasting 30 minutes was found. This means that it was discovered a time series which follows the same distribution in almost all its domain.

Tables 3.14, 3.15 and 3.16 represent the number of periods found with the same distribution as well its duration for streamwise, spanwise and vertical velocity, respectively.

K-S test, at 1/3 Hz

Duration's subset [min]	**Tower 37**	**Tower 20**	**Tower29**	
Direction	Southwest	Southwest	Southwest	Northeast
6	19	62	21	15
9	5	9	4	3
12	0	5	0	2
15	0	6	0	0
18	0	0	0	0
24	0	1	0	0

Table 3.14: K-S test, number of subset with different duration at 1/3 Hz in streamwise velocity.

K-S test, at 1/3 Hz

Duration subset [min]	**Tower 37**	**Tower 20**	**Tower29**	
Direction	Southwest	Southwest	Southwest	Northeast
6	25	60	15	12
9	4	18	2	5
12	0	7	3	4
15	0	3	0	1
18	0	0	0	0
21	0	1	0	0

Table 3.15: K-S test, number of subset with different duration at 1/3 Hz in spanwise velocity.

K-S test, at 1/3 Hz

Duration's subset [min]	**Tower 37**	**Tower 20**	**Tower29**	
Direction	Southwest	Southwest	Southwest	Northeast
6	14	38	13	17
9	11	25	6	14
12	2	12	5	3
15	3	6	1	0
18	0	4	0	1
21	1	0	1	0
24	1	1	0	0
27	0	1	0	1
30	0	1	0	0

Table 3.16: K-S test, Number of subset with different duration at 1/3 Hz in vertical component

K-S test - SW wind					
Date	**Tower**	**Height**	**U**	**V**	**W**
4 May	20	60	1×9min	1×6min	3×6min; 1×9min
	20	60	1×15min; 1×24min	1×6min; 2×12min	2×6min; 1×9min
	20	100	2×6min	1×6min	1×6min; 1×18min
	20	80 NW	1×15min	3×6min	2×6min; 2×9min; 1×12min
	20	80 SE	2×6min; 1×9min	2×6min	2×6min; 1×9min
	37	30	2×6min	1×6min	1×6min; 2×9min; 1×12min
6 May	29	100	1×9min	1×6min; 1×9min; 1×12min	1×24min
	29	100	4×6min	3×6min	2×6min; 1×9min
	29	30	0	0	1×6min; 1×9min; 1×12min
	29	80	2×6min	1×9min	2×9min; 1×12min
	29	80	4×6min	2×6min; 1×12min	2×6min; 2×12min
9 May	20	20	0	1×9min	1×6min
	20	40	3×6min	3×6min	1×6min; 1×12min; 1×30min
	20	60	1×12min	2×6min; 2×9min	2×6min; 2×9min
	37	40	1×6min; 1×9min; 1×12min	1×6min; 1×9min; 1×12min; 1×15min	1×6min; 2×12min; 1×18min
	37	60	0	2×6min	3×6min
	37	60	2×6min	2×6min; 1×12min	1×6min; 1×9min
	37	60	1×6min; 2×9min	2×6min; 1×9min	1×6min; 1×15min

K-S test - SW wind					
Date	**Tower**	**Height**	**U**	**V**	**W**
	20	30	0	1×6min	3×6min; 1×21min
	20	40	2×6min; 1×9min	1×6min; 1×12min	1×9min; 1×12min
	20	60	3×6min; 1×9min	1×6min; 1×9min	3×6min; 1×9min
10 May	20	100	3×6min	3×6min	1×12min
	20	80 SE	1×6min; 1×9min	5×6min	1×6min; 3×9min; 1×12min
	37	20	3×6min; 1×9min	1×6min; 1×9min	1×9min; 1×12min
	37	60	2×6min	1×6min	2×6min; 1×9min; 1×12min
11 May	20	60	1×9min	1×6min	2×6min
	20	80 SE	3×6min; 1×9min	3×6min	1×6min; 1×9min; 1×15min
12 May	20	80 NW	2×6min; 1×12min	3×6min; 1×9min	1×6min; 2×9min; 1×12min
	20	20	4×6min	1×6min; 2×9min	2×6min; 1×9min; 1×12min
	20	20	1×15min	2×6min; 1×9min	1×6min; 1×9min; 1×12min
	20	30	4×6min	3×6min; 1×9min	2×9min; 1×12min
	20	30	5×6min	2×6min	1×6min; 1×9min; 1×15min
13 May	20	100	2×6min	1×6min; 1×9min	1×6min; 2×9min; 1×12min
	20	80 NW	3×6min; 1×9min	1×6min; 2×9min	1×6min; 1×27min
	29	10	1×6min	2×6min; 1×9min	2×6min; 1×9min
	37	20	0	1×min; 1×15min	1×9min; 1×18min

K-S test - SW wind					
Date	**Tower**	**Height**	**U**	**V**	**W**
25 May	20	20	2×6min	3×6min; 1×9min	1×6min; 1×9min; 1×15min
	20	10	2×6min; 1×12min	2×6min	3×6min; 1×9min; 1×18min
	20	20	0	1×6min	1×6min
26 May	20	80 SE	1×6min	3×6min	2×6min; 1×15min
	29	20	4×6min	2×6min	1×6min; 1×9min; 2×12min
	29	80	1×6min; 1×9min	2×6min; 1×9min	1×6min
	37	30	3×6min	1×6min	3×6min; 1×9min
27 May	20	20	3×6min; 1×12min	2×6min; 1×9min	2×15min
28 May	37	40	1×6min; 1×15min	2×6min; 1×21min	1×6min; 1×15min
	37	60	3×6min	3×6min	1×6min; 1×9min
	20	20	2×6min	4×6min	1×6min; 1×9min; 1×15min
	20	30	2×6min; 1×15min	3×6min	0
29 May	20	40	2×6min	1×6min	1×9min
	20	40	3×6min	2×6min	1×9min
	20	60	2×6min; 1×9min	2×6min; 2×9min	1×6min; 1×9min; 1×15min; 1×24min
2 June	20	20	2×6min; 1×9min; 1×15min	2×6min; 1×9min	2×6min; 1×18min
14 June	20	30	3×6min	2×12min; 1×15min	1×9min
	29	60	4×6min	1×6min; 1×9min	1×6min; 2×9min

Table 3.17: Results for K-S test, in detail for each period, for SW wind

K-S test - NE wind					
Date	**Tower**	**Height**	**U**	**V**	**W**
3 May	29	30	0	1	2×6min; 1×12min
15 May	29	40	2×6min; 1×9min	1×6min; 3×9min	3×6min; 2×9min
20 May	29	30	2×6min	3×6min	3×6min
23 May	29	100	2×6min	5×6min	1×6min; 1×9min
	29	60	1×9min	1×6min; 1×15min	1×6min; 1×9min
	29	80	1×9min	1×6min	1×6min; 2×9min
24 May	29	20	3×6min; 1×9min	1×9min; 1×12min	1×9min; 1×12min
7 June	29	80	1×6min	1×6min; 3×12min	1×6min; 1×9min; 1×27min
8 June	29	100	2×6min	1×6min	2×6min; 1×9min
	29	30	2×6min; 1×9min	0	3×6min
10 June	29	40	2×6min; 1×12min	2×6min; 1×12min	1×6min; 1×9min

Table 3.18: Results for K-S test, in detail for each period, for NE wind

3.6 Nonstationary ratio

The nonstationarity ratio, proposed by Mahrt (1998), divides a time series into segments and compares the variability within all the time series with the variability within the segments (section 2.7). If the variability within all the time series is significantly larger than the variability within the segments (NR $>$ 2), the series is considered nonstationary.

In this test, each time series was divided into 30 subsets which means that in many cases the subsets were of 1 minute and in other cases they were 2 minutes.

Next, the results of the nonstationary ratio were taken from streamwise velocity of 65 time series that had been considered statically stationary by the first three criteria. In short, through the results, it was concluded that this test confirms that most of the periods considered stationary have in fact a non-stationary ratio below than 2 (figure 2.23. However, there were some exceptions where those ratio were so far from 2, such as:

- for NE winds, in tower 29:

  - on 3th May at 30 m height
  - on 7th June at 80 m height
  - on 10th June at 40 m

- for SW winds, in tower 29:
  - on 14th June at 60 m

- for SW wind, in tower 20:
  - on 13th May at 80 m
  - on 26th May at 20 m
  - on 27th May at 20 m

- for SW wind, in tower 37:
  - on 26th May at 20 m

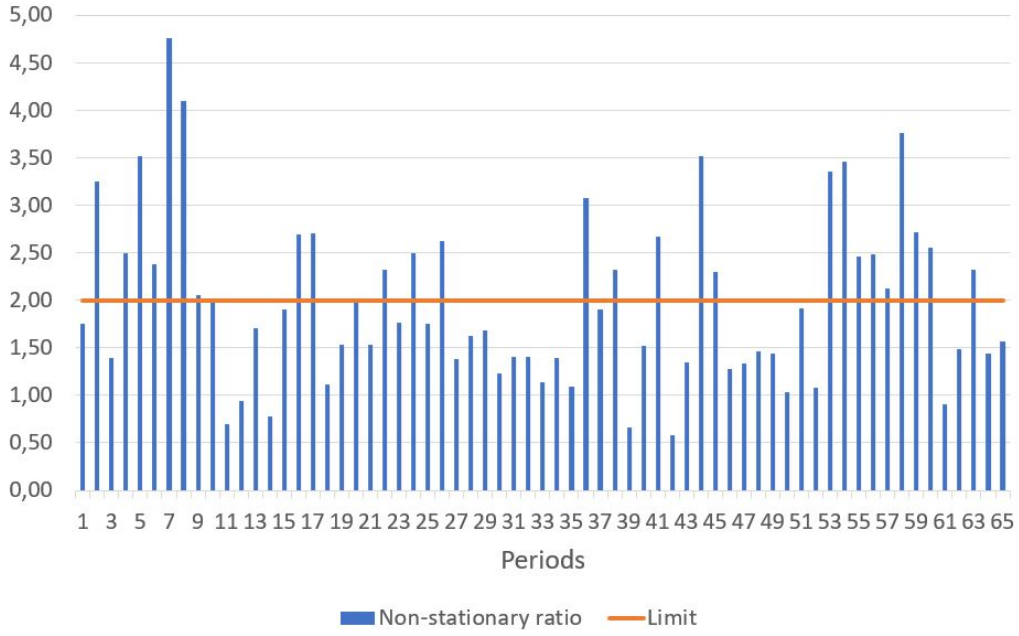

Figure 3.20: Results of nonstationary ratio for streamwise velocity

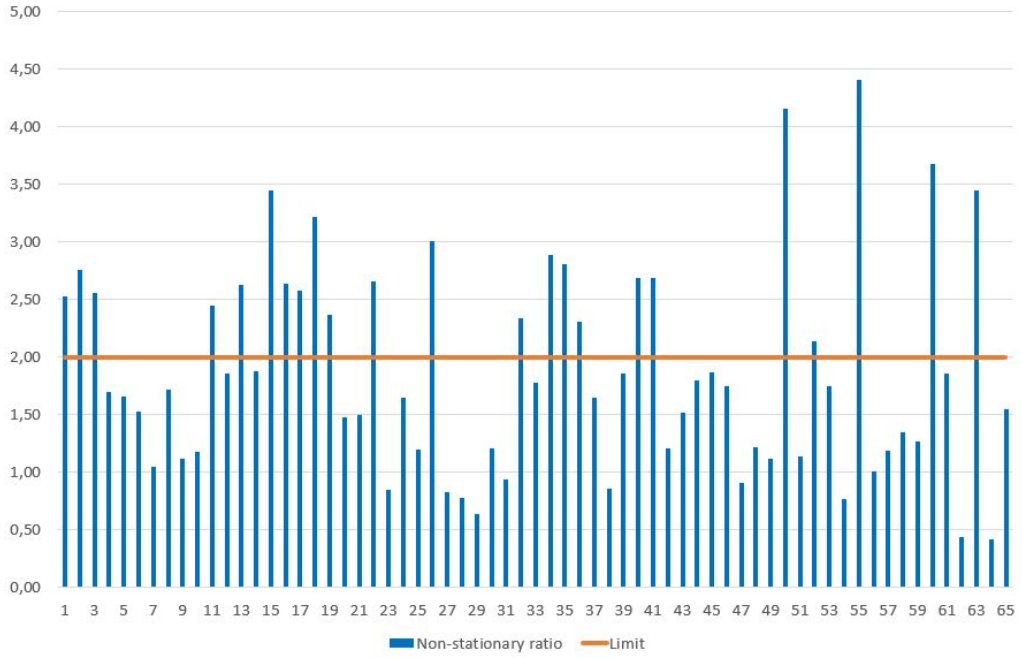

Figure 3.21: Results of nonstationary ratio for spanwise velocity

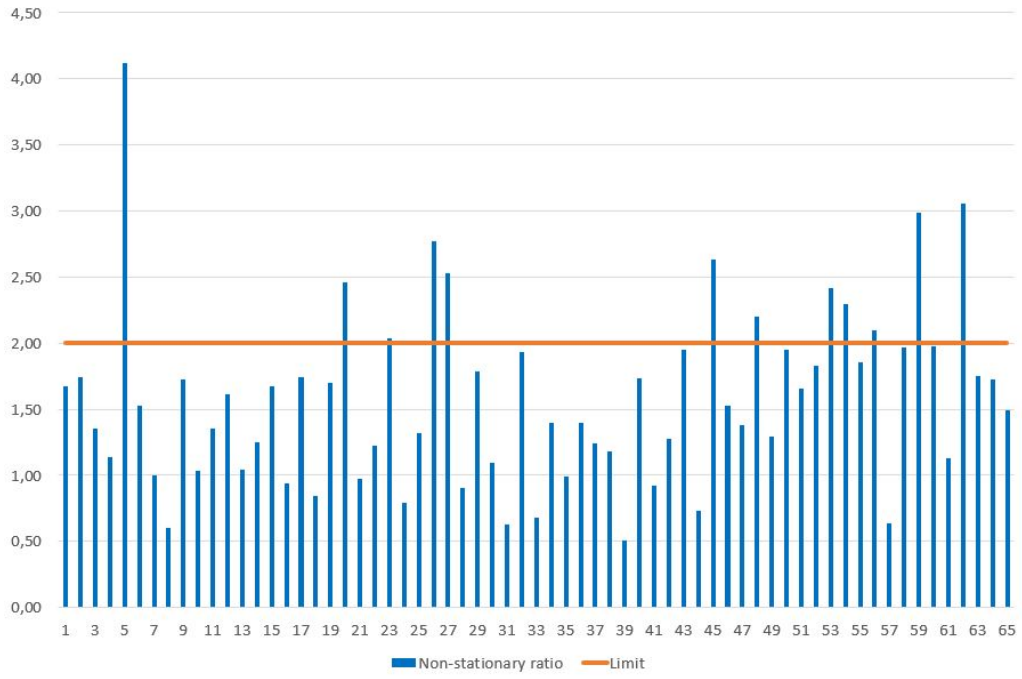

Figure 3.22: Results of nonstationary ratio for verical velocity

3.7 Summary

In this section, the periods that passed the first three steps of the procedure — wind direction, integral time scale and reverse arrangements test — are identified by the date and time they occurred and their duration is indicated (table 3.19). The results of the three alternatives for the last step — hypothesis test, K–S test and nonstationarity ratio — are also presented in detail here. From the wind direction criterion, 1049 periods were obtained to proceed the analysis. After using the integral time scale and the reverse arrangements, only 6% were considered, representing a total of 65 periods (figure 3.23 and table 3.19.

In terms of the total length of periods, most of the periods considered stationary do not last longer than 42 minutes, although 3 periods of about 1 hour have been found (figure 3.24). Figure 3.3 presents the days when stationary periods were found. On days 9, 10 and 13th May were the days with a higher number of stationary periods, with around 7 in each day. It should be noted that two stationary periods were found on the 6th of May, between 3h and 5h. They could be considered a single period if the wind direction had not changed for 4 seconds. These periods would form a period of 70 minutes, thus becoming the longest period found.

In the end, almost 41 hours of time series were considered stationary ($\approx 3\%$ of the total studied hours), most of which are between 20h and 9h (figure 3.25). The peak of stationary periods occurred between 23h and 00h and they were expected since stationary periods mostly occur in periods of the day when atmospheric conditions are neutral or stable, i.e. during the night.

Taking into account those periods, three alternatives methods were applied. Generally, the sizes of the periods found by the hypothesis test were larger than those found by the K-S test, due to the second one being more restricted. Still, the results between them are in agreement. However, there were some exceptions, such as:

- On the 9th of May, tower 20 at 60 m height, a 12 min period was the maximum found by hypothesis test while K-S test found a period with 15 min.
- On the 10th of May, tower 20 at 40 m height, the hypothesis test only found two 9-min periods, while the K-S test found one 12 min period.
- On the 10th of May, tower 20 at 10 m, one period of 6 min was found by the hypothesis test, while the K-S test assembled a period of 9 min.
- On the 13th of May, tower 20 at 100 m, two periods of 6 min were found with the hypothesis test, while the K-S test joined a period of 9 min.

The non-stationary ratio shows that it can be a good complement to the reverse arrangement test criterion. Most of the periods previously considered stationary were accepted. When comparing the NR with the hypothesis test and the K-S test, it does not exist any predominant relationship. The NR analyzed the total period, some of them with 60 minutes, while the hypothesis test and the K-S test analyzed small consecutive periods which lead to differences. Thus, there is a limitation of using the nonstationarity ratio to evaluate the stationarity on streamwise velocity. Further studies should consider the application of the nonstationarity ratio to the small periods.

Day	Tower	Height	Start time	End time	Wind direction
3 May	29	30	08:36	09:10	NE
4 May	20	80 NW	20:54	21:47	SW
	37	30	21:09	21:39	SW
	20	60	21:04	21:43	SW
	20	60	22:09	22:40	SW
	20	100	22:08	22:39	SW
	20	80 SE	22:09	22:40	SW
6 May	29	30	01:08	01:38	SW
	29	100	03:21	03:59	SW
	29	80	03:21	03:59	SW
	29	80	04:00	04:32	SW
	29	100	05:20	05:50	SW
9 May	37	60	19:03	19:42	SW
	37	60	21:36	22:33	SW
	20	20	22:09	22:44	SW
	20	40	22:11	22:44	SW
	37	40	23:25	00:04	SW
	20	60	23:23	00:00	SW
	37	60	23:25	00:05	SW
10 May	37	20	00:59	01:29	SW
	37	60	16:19	16:55	SW
	20	30	23:14	23:47	SW
	20	40	23:14	23:44	SW
	20	60	23:13	00:16	SW
	20	100	23:13	23:59	SW
	20	80 SE	23:13	00:18	SW
11 May	20	60	05:13	06:03	SW
	20	80 SE	05:13	05:53	SW
12 May	20	80 NW	23:01	23:32	SW
13 May	20	20	01:33	02:06	SW
	37	20	01:28	02:12	SW
	20	30	01:25	02:06	SW
	20	20	03:30	04:12	SW
	20	30	03:27	04:17	SW
	20	80 NW	08:20	08:52	SW
	20	100	09:40	10:14	SW
	29	10	23:43	00:19	SW
15 May	29	40	23:45	00:16	NE
20 May	29	30	08:14	08:48	NE
23 May	29	60	07:22	08:12	NE
	29	100	21:12	21:44	NE
	29	80	21:54	22:34	NE
24 May	29	20	00:19	00:52	NE
25May	20	20	23:43	00:15	SW

Day	Tower	Height	Start time	End time	Wind direction
26 May	29	20	00:27	01:01	SW
	29	80	00:33	01:12	SW
	37	30	07:48	08:22	SW
	20	80 SE	07:59	08:52	SW
	20	20	20:08	20:46	SW
	20	10	21:41	22:25	SW
27 May	20	20	00:03	00:38	SW
28 May	37	40	05:11	05:54	SW
	37	60	05:22	05:55	SW
29 May	20	40	00:56	01:27	SW
	20	20	01:34	02:11	SW
	20	30	03:35	04:06	SW
	20	40	03:34	04:05	SW
	20	60	03:30	04:18	SW
2 June	20	20	06:59	07:31	SW
7 June	29	80	18:33	19:08	NE
8 June	29	30	07:23	07:55	NE
	29	100	08:31	09:05	NE
10 June	29	40	04:09	04:45	NE
14 June	29	60	05:34	06:12	SW
	20	30	07:12	07:45	SW

Table 3.19: Stationary periods

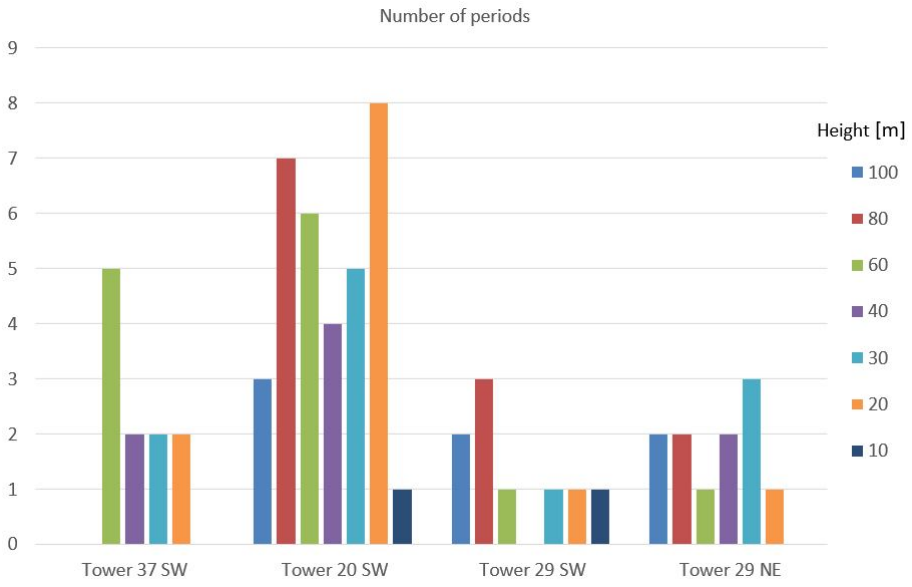

Figure 3.23: Number periods found after the first three steps

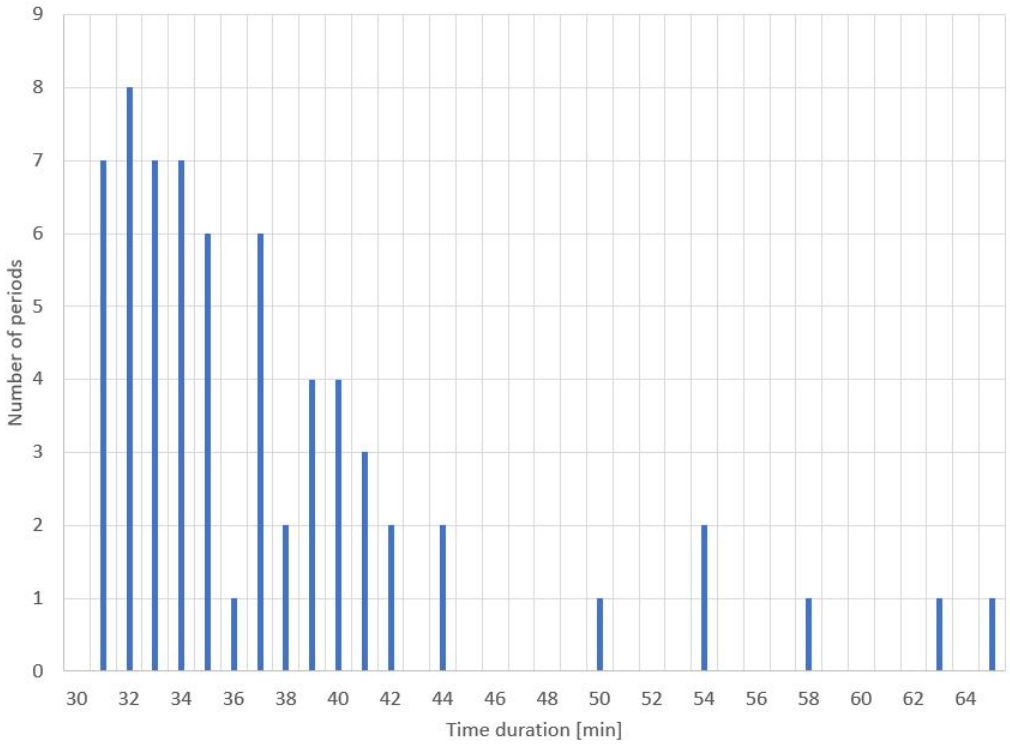

Figure 3.24: Periods characterized by its total duration

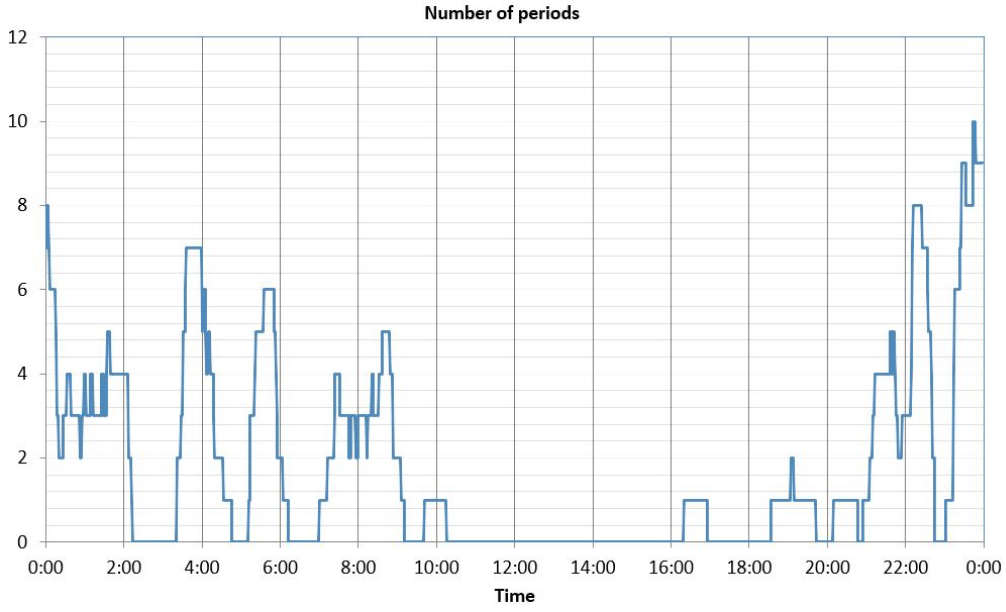

Figure 3.25: Daily time where the periods are distributed

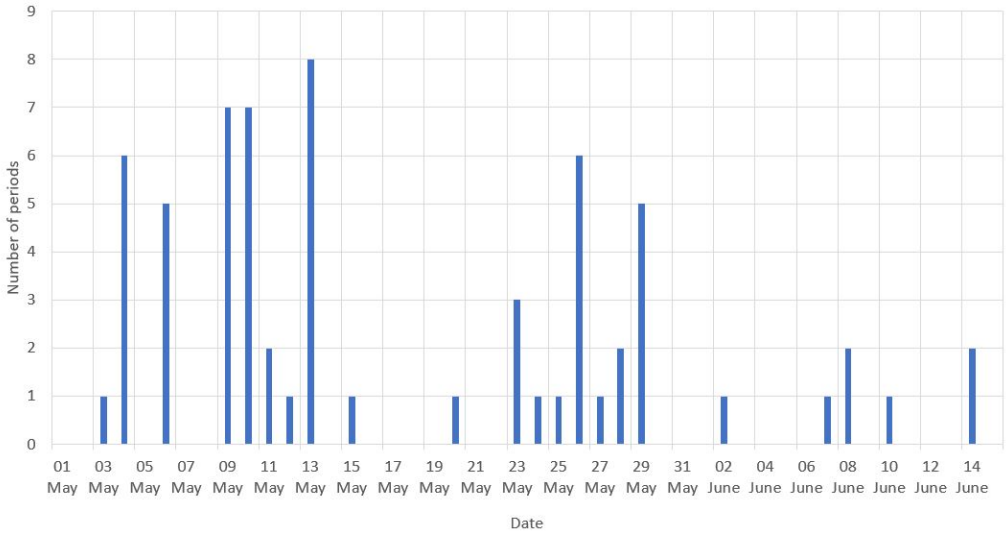

Figure 3.26: Days which stationary periods were found.

Date	Tower	Height	Hypothesis test	K-S test	NR
	20	60	2×9min	1×9min	1,98
	20	60	1×24min	1×15min; 1×24min	0,69
4 May	20	100	2×6min	2×6min	0,94
	20	80 NW	1×9min; 1×12min	1×15min	1,70
	20	80 SE	3×6min; 1×9min	2×6min; 1×9min	0,77
	37	30	1×9min	2×6min	2,06
	29	100	1×6min	1×9min	1,90
	29	100	4×6min; 2×9min; 1×12min	4×6min	2,7
6 May	29	30	2×6min	0	2,7
	29	80	2×6min; 1×12min	2×6min	1,12
	29	80	2×6min; 1×9min	4×6min	1,54
	20	20	1×6min	0	2,01
	20	40	2×6min	3×6min	1,53
	20	60	1×6min; 2×9min	1×12min	1,76
9 May	37	40	3×6min; 1×9min; 2×12min	1×6min; 1×9min; 1×12min	2,32
	37	60	1×6min	0	2,5
	37	60	1×6min; 1×12min	2×6min	1,76
	37	60	1×6min; 1×9min	1×6min; 2×9min	2,62

Date	Tower	Height	Hypothesis test	K-S test	NR
	20	30	1×6min; 1×9min; 1×12min	0	1,63
	20	40	1×9min; 1×12min	2×6min; 1×9min	1,68
	20	60	4×6min	3×6min; 1×9min	1,23
10 May	20	100	1×6min	3×6min	1,40
	20	80 SE	4×6min; 1×9min	1×6min; 1×9min	1,14
	37	20	5×6min	3×6min; 1×9min	1,38
	37	60	1×9min	2×6min	1,41
11 May	20	60	1×6min; 2×9min	1×9min	1,39
	20	80 SE	1×6min; 2×9min	3×6min; 1×9min	1,10
12 May	20	80 NW	2×6min; 1×9min; 1×18min	2×6min; 1×12min	3,08
	20	20	1×6min	4×6min	1,90
	20	20	1×18min	1×15min	2,32
	20	30	2×6min; 1×9min	4×6min	1,52
13 May	20	30	1×6min; 2×9min	5×6min	2,67
	20	100	2×6min	2×6min	0,59
	20	80 NW	2×9min	3×6min; 1×9min	3,51
	29	10	1×6min	1×6min	1,34
	37	20	2×9min	0	0,66
25 May	20	20	2×6min; 1×9min	2×6min	1,91

Date	Tower	Height	Hypothesis test	K-S test	NR
	20	10	1×6min; 1×9min; 1×15min	2×6min; 1×12min	1,08
	20	20	1×6min	0	3,36
26 May	20	80 SE	2×6min; 1×9min	1×6min	2,49
	29	20	3×6min; 1×12min	4×6min	2,46
	29	80	2×6min	1×6min; 1×9min	2,12
	37	30	2×6min	3×6min	3,46
27 May	20	20	3×6min; 1×18min	3×6min; 1×12min	3,77
28 May	37	40	1×6min; 1×9min; 1×15min	1×6min; 1×15min	2,72
	37	60	0	3×6min	2,56
	20	20	1×9min	2×6min	0,91
	20	30	1×6min; 2×18min	2×6min; 1×15min	1,49
29 May	20	40	3×6min	2×6min	2,32
	20	40	4×6min	3×6min	1,45
	20	60	2×6min;1×9min	2×6min;1×9min	1,56
2 June	20	20	2×6min; 1×9min 1×15min	2×6min; 1×9min 1×15min	1,75
14 June	20	30	2×6min;1×9min	3×6min	2,38
	29	60	1×6min;1×9min	4×6min	4,76

Table 3.20: Results in detail for each period, for SW wind

Date	Tower	Height	Hypothesis test	K-S test	NR
3 May	29	30	0	0	4,10
15 May	29	30	2×6min	2×6min 1×9min	2,30
20 May	29	40	2×6min 2×9min	2×6min	1,28
23 May	29	60	1×9min 1×12min	2×6min	1,44
	29	80	1×9min	1×9min	1,46
	29	100	2×6min 1×9min	1×9min	1,34
24 May	29	20	2×6min 1×9min	3×6min 1×9min	1,04
7 June	29	80	1×6min 1×9min	1×6min	3,25
8 June	29	30	2×6min 2×9min	2×6min	2,50
	29	100	1×6min	2×6min 1×9min	1,39
10 June	29	40	1×24min	2×6min 1×12min	3,51

Table 3.21: Results in detail for each period, for NE wind

3.7.1 Stationary periods

The days with more stationary periods were comprised between the 4th and 9th of May and also the 26th and 29th of May. In this section, it are presented details and some reasons which justify why those periods were selected. On May 4, it were found 3 time intervals which met in time and towers, even more, they contained 24 min subsets of same average and distribution. Table 3.22 describe some features on those periods.

Tower	Height [m]	Average [m/s]	Turbulence intensity	Start time	End time
Twr20	60	5,766	0,114	22:09	22:40
Twr20	80	5,746	0,10	22:08	22:39
Twr20	100	5,669	0,101	22:09	22:40

Table 3.22: Day 4 May: details of periods

Another day selected was 9 of May, those periods were able to join subsets with 15 and 24 min with same average and distribution although has been found in different towers.

Tower	Height [m]	Average [m/s]	Turbulence intensity	Start time	End time
Twr37	40	6,546	0,112	23:25	00h04
Twr20	60	7,023	0,115	23:23	00h00
Twr37	60	6,698	0,114	23:25	00h05

Table 3.23: Day 9 May: details of periods

In 26 of May, 6 periods were considered stationary and the alternatives test found subsets with 24 min. However they do not coincide in time even in tower. But on this day, all towers registered stationary conditions.

Tower	Height [m]	Average [m/s]	Turbulence intensity	Start time	End time
Twr29	20	1,922	0,107	00:27	01:01
Twr29	80 NW	2,335	0,162	00:33	01:12
Twr37	30	4,714	0,098	07:48	08:22
Twr20	80 SE	5,025	0,134	07:59	08:52
Twr20	20	7,423	0,074	20:08	20:46
Twr20	10	5,722	0,063	21:41	22:25

Table 3.24: Day 26 May: details of periods

Finally, on the 29th of May, between 1h00 and 2h00 and from 03h30 to 04h30, where it was verified periods placed in three heights, between 20 and 60 m height. On this day, 3 periods are coincide in same tower (tower 20), composed with 15 and 18 min subsets.

Tower	Height [m]	Average [m/s]	Turbulence intensity	Start time	End time
Twr20	30	3,660	0,097	03:35	04:06
Twr20	40	3,78425	0,094	03:34	04:05
Twr20	60	4,068	0,119	03:30	04:18

Table 3.25: Day 29 May: details of periods

Chapter 4

Conclusions and future work

The main conclusions drawn from this thesis are presented in this chapter, as well as some suggestions and recommendations for future development of this work.

4.1 Conclusions

In order to find stationary periods in the measurements taken during the IOP of the Perdigão 2017 experiment, an algorithm consisting in the consecutive application of three filters was established. The wind direction criterion was applied with the objective of finding periods of time in which the wind flow was always normal to the ridges (SW and NE winds). Time series with the integral time scale, τ_ϕ, above 100 s were rejected, eliminating periods affected by large-scale motions and unstable conditions. Thus, subsets of duration $deltast > 2\tau_\phi$ provided independent samples that were analyzed in the reverse arrangement test, at a 95% confidence level.

Subsequently, three statistical alternatives were used to evaluate consecutive averaged sub-records. These were the Hypothesis test, to test if they had the same average, the K–S test, to test if they had the same distribution, and the nonstationary ratio.

In the total of 45 days measurements, some conclusion drawn from the analyzed data about wind direction criterion:

- 1049 periods of time with relatively steady ($\pm$ 30°) southwest and northeast winds;
- Both tower 37 and 20 measured about the same periods for each height;
- Higher numbers of stationary periods were found, when it was analyzed upstream flow than in the downstream flow;

One consequence of the instability flow motions of the large scales are that they produce signals with low frequency. The criteria of the integral time scale less than 100 seconds eliminated those periods and rejected 90% of the total periods. Periods belonging to the entire day were rejected by the criterion, i.e. did not exclude only nocturnal or diurnal periods. In addition, the criterion eliminated very long periods, restricting the maximum duration to 87 minutes. After the reverse arrangements test, 65 stationary periods were found. The majority of them were between sunset and sunrise, most of them between 22h and 8h.

A duration larger than 30 min was a requirement to the application of the three alternative methods. The time series analyzed were applied at 95% confidence level, and last between 30 and 60 min. In practice, the 18 Hz, 3 min samples were not really independent, resulting in periods with the same average with the maximum duration of 6 minutes, after the hypothesis test. Knowing that the integral times scales were about 50 seconds, diverse sample rates were testes, up to 1/3 Hz, getting larger periods with the same average and with the same distribution. With the lower sample rates, 24 min periods with the same distribution of streamwise velocity were found, even more in vertical component up to 30 min subsets.

The days with more stationary periods were comprised between the 4th and 13th of May and also the 26th and 29th of May. Especially, for NE winds in the north ridge, the 23rd of May had the most stationary periods between 21h00 and 23h00, mainly at 100 and 80 m height. For SW winds in the south ridge, the 4th of May between 21h00 and 23h00 presented stationary conditions, at 60, 80, 100 m height. Also, on the 9th of May between 21h30 and 00h00, where was found 3 periods of 12 min with same average and distribution. Finally, on the 29th of May, between 1h00 and 2h00 and from 03h30 to 04h30, where it was verified periods placed in three heights, between 20 and 60 m height.

4.2 Future work

- It would be useful to study data already available from other towers and measuring instruments, to provide an even better view of the experiment;
- Analysis of data from more sites — preferably before the ridges — would allow to determine better the stratification of the flow;
- A joint analysis of the influence of the size of the elementary periods and the sample rate considered in the hypothesis and K-S tests, considering the integral length scale of each case, to have periods with really independent samples.

Bibliography

Travis W Beck, Terry J Housh, Joseph P Weir, Joel T Cramer, Vassilios Vardaxis, Glen O Johnson, Jared W Coburn, Moh H Malek, and Michelle Mielke. An examination of the runs test, reverse arrangements test, and modified reverse arrangements test for assessing surface emg signal stationarity. *Journal of neuroscience methods*, 156(1-2):242–248, 2006.

Julius S Bendat and Allan G Piersol. *Random data: analysis and measurement procedures*. Wiley, 2000.

Carlos Alberto Madureira da Silva. Computational Study of Atmospheric Flows Over Perdigao: Terrain Resolution and Domain Size. Master's thesis, University of Porto, 2018.

Nelson L. Dias, Marcelo Chamecki, Akemi Kan, and Cristhiane M. P. Okawa. A study of spectra, structure and correlation functions and their implications for the stationarity of surface-layer turbulence. *Boundary-Layer Meteorology*, 110(2):165–189, Feb 2004. ISSN 1573-1472. doi: 10.1023/A:1026067224894. URL https://doi.org/10.1023/A:1026067224894.

H.J.S. Fernando, J. Mann, J.M.L.M. Palma, J.K. Lundquist, R.J. Barthelmie, M. BeloPereira, W.O.J. Brown, F.K. Chow, T. Gerz, C.M. Hocut, P.M. Klein, L.S. Leo, J.C. Matos, S.P. Oncley, S.C. Pryor, L. Bariteau, T.M. Bell, N. Bodini, M.B. Carney, M.S. Courtney, E.D. Creegan, R. Dimitrova, S. Gomes, M. Hagen, J.O. Hyde, S. Kigle, R. Krishnamurthy, J.C. Lopes, L. Mazzaro, J.M.T. Neher, R. Menke, P. Murphy, L. Oswald, S. Otarola-Bustos, A.K. Pattantyus, C. Veiga Rodrigues, A. Schady, N. Sirin, S. Spuler, E. Svensson, J. Tomaszewski, D.D. Turner, L. van Veen, N. Vasiljević, D. Vassallo, S. Voss, N. Wildmann, and Y. Wang. The perdigão: Peering into microscale details of mountain winds. *Bulletin of the American Meteorological Society*, 0(0):null, 2018. doi: 10.1175/BAMS-D-17-0227.1. URL https://doi.org/10.1175/BAMS-D-17-0227.1.

Rui Campos Guimarães and José A Sarsfield Cabral. Estatística–mcgraw-hill, 2011.

Jagadish Chandran Kaimal and John J Finnigan. *Atmospheric boundary layer flows: their structure and measurement*. Oxford university press, 1994.

Donald H. Lenschow and B. Boba Stankov. Length scales in the convective boundary layer. *Journal of the Atmospheric Sciences*, 43(12):1198–1209, 1986. doi: 10.1175/1520-0469(1986)043⟨1198:LSITCB⟩2.0.CO;2. URL https://doi.org/10.1175/1520-0469(1986)043<1198:LSITCB>2.0.CO;2.

Larry Mahrt. Flux sampling errors for aircraft and towers. *Journal of Atmospheric and Oceanic technology*, 15(2):416–429, 1998.

Jakob Mann. New european wind atlas, 2015. URL https://newanewsletter.wordpress.com/category/perdigao-campaign/.

NCAR/UCAR. Earth observing laboratory, 2016. URL https://www.eol.ucar.edu/field_projects/perdigao.

Ying Pan and Edward G Patton. On determining stationary periods within time series. *Journal of Atmospheric and Oceanic Technology*, 34(10):2213–2232, 2017.

Sidney Siegal. *Nonparametric statistics for the behavioral sciences*. McGraw-hill, 1956.

Nikolai V Smirnov. Estimate of deviation between empirical distribution functions in two independent samples. *Bulletin Moscow University*, 2(2):3–16, 1939.

P. A. Taylor and H. W. Teunissen. The askervein hill project: Overview and background data. *Boundary-Layer Meteorology*, 39(1):15–39, Apr 1987. ISSN 1573-1472. doi: 10.1007/BF00121863. URL https://doi.org/10.1007/BF00121863.

Dave Trindade. The reverse arrangement test: A simple procedure for detecting trends in equipment reliability, 1995. URL https://www.trindade.com/Artwork20199520RAT20Boston.pdf.

José Miguel Almeida Vilaça. Analysis of atmospheric conditions: Data quality and stationarity in perdigao. Master's thesis, University of Porto, 2018.

Alexandra Witze. World's largest wind-mapping project spins up in portugal, 2017. URL https://www.nature.com/news/world-s-largest-wind-mapping-project-spins-up-in-portugal-1.21481.

Appendices

Appendix A

Devices location

Nº Tower: 37/rsw06
Location: 33087.97 E 4686.07 N

ID Code	Equipment	Height (agl)	Orientation
DSA513715	3D Sonic anemometer	57.15 m	149.34º
DSA483719	3D Sonic anemometer	40.19 m	141.85º
DSA503721	3D Sonic anemometer	30.21 m	142.67º
DSA493736	3D Sonic anemometer	20.36 m	143.87º
DSA4737.3	3D Sonic anemometer	10.3 m	154.14º
D093712	Data-logger	12 m	-

Table A.1: Devices used in tower 37

Nº Tower: 20/tse04
Location: 33394.18 E 4258.87 N

ID Code	Equipment	Height (agl)	Orientation
DSA172000	3D Sonic anemometer	100 m	136.33 º
DSA162078	3D Sonic anemometer	78 m	135.42 º
DSA152060	1 3D Sonic anemometer	60 m	134.88 º
DSA142040	3D Sonic anemometer	40 m	134.57 º
DSA132030	3D Sonic anemometer	30 m	135 º
DSA122020	3D Sonic anemometer	20 m	135.05 º
DSA112010	3D Sonic anemometer	10 m	137.73 º
D032012	Data-logger	12 m	-

Table A.2: Devices used in tower 20

Nº Tower: 29/tse13
Location: 34533.6 E 5112.01 N

ID Code	Equipment	Height (agl)	Orientation
DSA412904	3D Sonic anemometer	97.04 m	137.3 º
DSA402997	3D Sonic anemometer	79.97 m	135.36 º
DSA392915	3D Sonic anemometer	60.15 m	133.47 º
DSA382903	3D Sonic anemometer	40.03 m	131.75 º
DSA372912	3D Sonic anemometer	30.12 m	131.15 º
DSA362902	3D Sonic anemometer	20.02 m	129.91 º
DSA352902	3D Sonic anemometer	10.02 m	129.57 º
D072912	Data-logger	12 m	-

Table A.3: Devices used in tower 29

Appendix B

Results after direction criterion

Nº Tower: 37/rsw06

Height agl [m]	Number of periods	Wind direction	Total
60	47		
40	47		
30	53	**Southwest**	**227**
20	48		
10	32		

Table B.1: Periods found in tower 37

Nº Tower: 20/tse04

Height agl [m]	Number of periods	Wind direction	Total
100	44		
80 - SE	47		
80 - NW	50		
60	50	**Southwest**	**353**
40	55		
30	48		
20	46		
10	13		

Table B.2: Periods found in tower 20

Nº Tower: 29/tse13

Height agl [m]	Number of periods	Wind direction	Total
100	27		
80	25		
60	26		
40	23	**Southwest**	**132**
30	22		
20	7		
10	2		
100	60		
80	66		
60	51		
40	57	**Northeast**	**337**
30	59		
20	42		
10	2		

Table B.3: Periods found in tower 29

	Towers		
Height agl [m]	**37/rsw06**	**20/tse04**	**29/tse13**
100	-	2	1
80	-	4	1
60	4	2	1
40	4	2	1
30	4	2	1
20	3	1	1
10	3	2	1

Table B.4: Number of invalid periods for the respective tower and height.

Appendix C

Results after the integral time scale criterion

Spanwise velocity

Height agl [m]	**Tower 37**	**Tower 20**	**Tower29**	
Direction	Southwest	Southwest	Southwest	Northeast
100	0	6	3	5
80	0	18	5	5
60	10	8	4	2
40	7	7	6	5
30	8	6	4	4
20	4	10	2	3
10	2	2	2	0

Table C.2: Periods with $\tau_v \leq 100$ seconds

Sreamwise velocity

Height agl [m]	**Tower 37**	**Tower 20**	**Tower29**	
Direction	Southwest	Southwest	Southwest	Northeast
100	0	10	4	9
80	0	24	5	13
60	13	11	4	6
40	10	11	6	10
30	11	9	5	8
20	7	12	2	4
10	3	3	2	0

Table C.1: Periods with $\tau_u \leq 100$ seconds

Vertical velocity

Height agl [m]	**Tower 37**	**Tower 20**	**Tower29**	
Direction	Southwest	Southwest	Southwest	Northeast
100	0	5	3	5
80	0	15	5	5
60	10	7	4	2
40	7	6	5	4
30	8	5	4	4
20	4	9	2	3
10	2	2	2	0

Table C.3: Periods with $\tau_w \leq 100$ seconds

Appendix D

Results after the reverse arrangements test

Streamwise velocity

Height agl [m]	**Tower 37**	**Tower 20**	**Tower29**	
Direction	Southwest	Southwest	Southwest	Northeast
100	0	5	1	3
80	0	14	3	2
60	7	7	1	2
40	4	5	3	2
30	4	4	3	2
20	3	7	1	2
10	0	2	1	0

Table D.1: Periods which were accepted by the reverse arrangements test for the streamwise velocity

Spanwise velocity

Height agl [m]	**Tower 37**	**Tower 20**	**Tower29**	
Direction	Southwest	Southwest	Southwest	Northeast
100	0	4	1	3
80	0	9	3	2
60	7	6	1	2
40	3	3	2	1
30	3	4	2	2
20	2	7	1	2
10	0	1	1	0

Table D.2: Periods which were accepted by reverse arrangements test for the spanwise velocity

Vertical velocity

Height agl [m]	**Tower 37**	**Tower 20**	**Tower29**	
Direction	Southwest	Southwest	Southwest	Northeast
100	0	3	1	2
80	0	7	3	2
60	5	6	1	1
40	2	3	0	1
30	2	4	1	1
20	2	7	1	1
10	0	1	1	0

Table D.3: Periods which were accepted by the reverse arrangements test for the all velocity components